American Journal of Botany

RESEARCH ARTICLE

Phylogeny and diversification history of the large Neotropical genus *Philodendron* (Araceae): Accelerated speciation in a lineage dominated by epiphytes

Dubán Canal[1,3], Nils Köster[1], Katy E. Jones[1], Nadja Korotkova[1], Thomas B. Croat[2], and Thomas Borsch[1]

Manuscript received 24 November 2017; revision accepted 17 April 2018.

[1] Botanischer Garten und Botanisches Museum Berlin, Freie Universität Berlin, Königin-Luise-Straße 6-8, D-14195 Berlin, Germany

[2] Missouri Botanical Garden, Monsanto Research Building, P.O. Box 299, St. Louis, Missouri 63166, USA

[3] Author for correspondence (e-mail: dubancanal@gmail.com)

Citation: Canal, D., N. Köster, K. E. Jones, N. Korotkova, T. B. Croat, and T. Borsch. 2018. Phylogeny and diversification history of the large Neotropical genus *Philodendron* (Araceae): Accelerated speciation in a lineage dominated by epiphytes. *American Journal of Botany* 105(6): 1035–1052.

doi:10.1002/ajb2.1111

PREMISE OF THE STUDY: *Philodendron* is a large genus of ~560 species and among the most conspicuous epiphytic components of Neotropical forests, yet its phylogenetic relationships, timing of divergence, and diversification history have remained unclear. We present a comprehensive phylogenetic study for *Philodendron* and investigate its diversification, including divergence-time estimates and diversification rate shift analyses.

METHODS: We performed the largest phylogenetic reconstruction for *Philodendron* to date, including 125 taxa with a combined dataset of three plastid regions (*petD*, *rpl16*, and *trnK/matK*). We estimated divergence times using Bayesian evolutionary analysis sampling trees and inferred shifts in diversification rates using Bayesian analysis of macroevolutionary mixtures.

KEY RESULTS: We found that *Philodendron*, its three subgenera, and the closely related genus *Adelonema* are monophyletic. Within *Philodendron* subgenus *Philodendron*, 12 statistically well-supported clades are recognized. The genus *Philodendron* originated ~25 mya and a diversification rate upshift was detected at the origin of subgenus *Philodendron* ~12 mya.

CONCLUSIONS: *Philodendron* is a species-rich Neotropical lineage that diverged from *Adelonema* during the late Oligocene. Within *Philodendron*, the three subgenera currently accepted are recovered in two lineages: one contains the subgenera *Meconostigma* and *Pteromischum* and the other contains subgenus *Philodendron*. The lineage containing subgenera *Meconostigma* and *Pteromischum* underwent a consistent diversification rate. By contrast, a diversification rate upshift occurred within subgenus *Philodendron* ~12 mya. This diversification rate upshift is associated with the species radiation of the most speciose subgenus within *Philodendron*. The sections accepted within subgenus *Philodendron* are not congruent with the clades recovered. Instead, the clades are geographically defined.

KEY WORDS Araceae; divergence-time estimates; diversification rate shifts; museum and cradle models; Neotropics; *Philodendron*.

The Neotropical region (tropical America) is the most species-rich area on Earth, comprising ~37% of extant seed plants (Antonelli and Sanmartín, 2011; Hughes et al., 2013). The origin of this exceptional diversity has attracted the attention of biogeographers, plant evolutionary biologists, and systematists (Hughes et al., 2013; Pennington et al., 2015). The existence of angiosperm lineages that originated during the Eocene (or earlier) led to the hypothesis that Neotropical forests are "museums" of diversity, which have accumulated species over a long period (Davis et al., 2005; Couvreur et al., 2011; Lohmann et al., 2013; Pennington et al., 2015; Schneider and Zizka, 2017). The rationale for this hypothesis is that Neotropical forests are considered to have constituted stable environments that allowed the accumulation of species while extinction rates were low. In contrast, the discovery of lineages that diversified relatively recently from the late Miocene onward supports the hypothesis that the Neotropical forests are more likely "cradles" where species have evolved at high rates (Richardson et al., 2001; Kay et al., 2005; Erkens et al., 2007; Särkinen et al., 2007; Drew and Sytsma, 2013; Neupane et al., 2017). However, the "museum" and "cradle" models are not mutually exclusive, and the high species diversity in

the Neotropics may be explained by high species turnover at different geological periods (McKenna and Farrell, 2006; Koenen et al., 2015). Therefore, this species diversity in Neotropical lineages may be explained by episodic bursts of high speciation and extinction rates through time (Pennington et al., 2015).

The genus *Philodendron* Schott (Araceae) is among the most characteristic epiphytic components of the Neotropical rainforests, in terms of both species diversity and abundance of individuals (Croat, 1997). With ~560 currently accepted species and an estimated total of ~700 species (Govaerts et al., 2017), *Philodendron* is the second largest genus of the aroid family after *Anthurium* Schott, with >1000 species (Carlsen and Croat, 2013). In the Araceae, *Philodendron* is one of the most diverse genera in terms of both leaf morphology and life forms—the genus includes terrestrials, vines, hemiepiphytes, and epiphytes (Croat, 1997; Croat et al., 2010). Despite the significant contribution of *Philodendron* to vascular epiphyte diversity in the Neotropics, phylogenetic studies to date have been based on limited taxon sampling and have resulted in partially resolved phylogenetic trees (Barabé et al., 2002; Gauthier et al., 2008; Loss-Oliveira et al., 2016).

Based on the phylogenetic studies of *Philodendron* available to date, which have used plastid DNA (partial *rpl16* intron, *matK* gene, *trnL* intron, and *trnL-trnF* spacer sequences) and nuclear ribosomal DNA (external transcribed spacer [ETS] and internal transcribed spacer [ITS]), two contrasting hypotheses have been proposed with regard to the monophyly of the genus and its position with respect to the closely related genera *Adelonema* Schott and *Homalomena* Schott. The genus *Adelonema* was recently resurrected (Wong et al., 2016) and comprises 16 Neotropical species formerly assigned to *Homalomena*. The latter is therefore now considered a tropical Asian genus. The phylogenetic trees inferred by Barabé et al. (2002; based on the *trnL* intron and *trnL-trnF* spacer), Gauthier et al. (2008; based on the *rpl16* intron), Wong et al. (2013; based on the ITS), and Wong et al. (2016; using ITS and *matK*) resolved subgenus *Pteromischum* as sister to *Adelonema*. In contrast, the phylogenetic trees inferred by Gauthier et al. (2008; based on ETS and ITS) and Loss-Oliveira et al. (2016; based on ETS, *matK*, *trnL*, and *trnL-trnF*) recovered the entire genus *Philodendron* as a monophyletic group sister to *Adelonema*.

Morphological and anatomical characters of the inflorescences have been used for the infrageneric circumscription of *Philodendron* (Croat, 1997). Androecial characters were mostly used at the subgeneric level, and gynoecial characters at the sectional level (Engler, 1899; Mayo, 1988, 1989; Croat, 1997). There are three subgenera in *Philodendron* that are morphologically and anatomically distinct from each other: subgenus *Meconostigma* Engl., subgenus *Philodendron* Schott, and subgenus *Pteromischum* (Schott) Mayo (Mayo, 1986; Croat, 1997; Croat et al., 2016). The relationships among them, however, remain uncertain (Gauthier et al., 2008; Loss-Oliveira et al., 2016). *Philodendron* subgenus *Meconostigma*, which has recently been shown to be monophyletic, comprises 21 mostly terrestrial species distributed in Amazonia, the Mata Atlântica, and the Cerrado (Mayo, 1988; Braucks Calazans et al., 2014; Fig. 1). *Philodendron* subgenus *Pteromischum* comprises two sections (sect. *Fruticosa* Grayum and sect. *Pteromischum* [Schott] Engl.) and includes 82 vine species distributed mostly in Central America and Amazonia (Grayum, 1996; Croat, 1997; Calazans and Sakuragui, 2013; Barbosa and Sakuragui, 2014; Fig. 1). With 457 currently accepted species and an estimated total of >600 species, *Philodendron* subgenus *Philodendron* accounts for ~85% of the species diversity of the genus, mainly distributed in the Andes, Amazonia, Central America, and the Chocó ecoregion (Fig. 1). Members of subgenus *Philodendron* are predominantly epiphytic (including facultative epiphytes and hemiepiphytes), although it is often difficult to attribute *Philodendron* species unequivocally to the epiphytic life form (Zotz, 2013). The currently accepted classification within subgenus *Philodendron* consists of 10 sections, 12 subsections, and 11 series mainly characterized by leaf morphology in combination with the number of locules per ovary, the number of ovules per locule, the type of placentation, and the shape of the style (Croat, 1997, 2013; Köster and Croat, 2011). The monophyly of subgenus *Philodendron* is

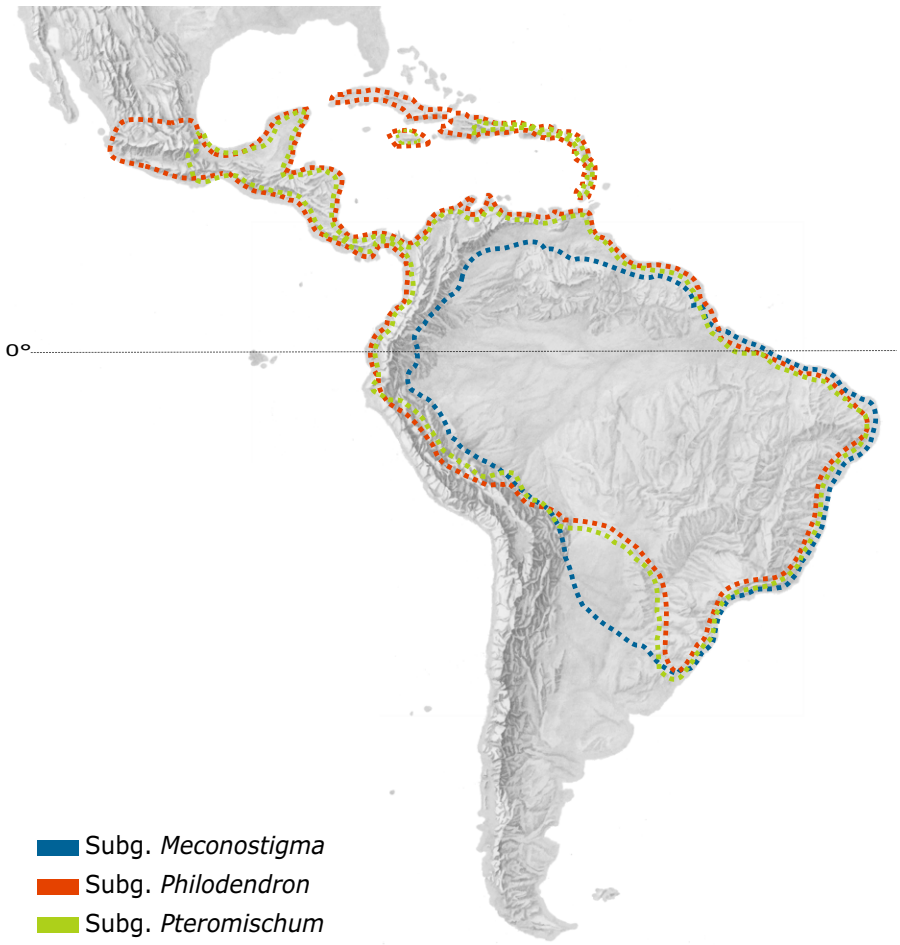

FIGURE 1. Distribution area of each of the three subgenera of *Philodendron*. (Relief source: Herwig G. Schutzler, 1970.)

unclear; the phylogenetic trees inferred from analyses of ETS and ITS of 55 species recovered subgenus *Philodendron* as only a weakly supported monophyletic group (Gauthier et al., 2008).

The origin and divergence times of *Philodendron* need further investigation. According to the fossil-calibrated phylogenetic tree inferred for the family Araceae (Nauheimer et al., 2012), the clade including *Adelonema*, *Furtadoa* M. Hotta, *Homalomena*, and *Philodendron* diverged from its sister clade ~25 mya (95% highest posterior density [HPD]: 11.8–39.4) in the late Oligocene, and *Philodendron* originated ~20.5 mya (95% HPD: 9.2–33.2) in the early Miocene. Loss-Oliveira et al. (2016) used fixed average substitution rates of plastid coding regions estimated in monocots to infer ages of *Philodendron*, and suggested that *Homalomena* diverged from its sister clade comprising *Adelonema* and *Philodendron* in the middle to late Miocene (95% HPD: 9.2–12.8, median age not given) and that *Philodendron* originated ~8.6 mya (95% HPD: 6.8–12.1). In both of the above studies, however, the nodes critical for inferring the closest extant relatives of *Philodendron* are not well supported.

Well-resolved, robustly supported, and time-calibrated phylogenetic trees of species-rich Neotropical lineages such as *Philodendron* are relevant to better understand its origin and species radiation, and will provide the comparative basis to gain insights into the evolution of Neotropical plant lineages. Therefore, the goal of this investigation was to generate a well-resolved and statistically supported phylogeny of *Philodendron* based on a broad taxon sampling that could also be used in divergence-time analyses. Consequently, we generated a dataset of three plastid DNA regions for 125 taxa within the genus *Philodendron* to specifically (1) assess the monophyly of *Philodendron* and resolve relationships both between the genus *Philodendron* and the closely related genera *Adelonema* and *Homalomena* and between the subgenera within *Philodendron* (*Meconostigma*, *Philodendron*, and *Pteromischum*); (2) assess the relationships down to species level, in particular within the large subgenus *Philodendron*; and (3) estimate relative timing and diversification rate shifts throughout the history of *Philodendron*. In addition, we compare our findings in *Philodendron* with other Neotropical plant lineages and discuss them in the context of the scenarios for species diversification in the Neotropics (museum and cradle models; Koenen et al., 2015; Pennington et al., 2015).

MATERIAL AND METHODS

Taxon sampling, DNA extraction, amplification, sequencing, and alignment

The taxonomic treatment by Krause (1913) was the last complete revision of *Philodendron*. Therefore, we sampled as widely as possible across the genus, following regional taxonomic treatments and comparative studies of selected species groups (Mayo, 1991; Grayum, 1996; Croat, 1997; Köster and Croat, 2011). We covered both a broad range of morphological variation as well as the entire geographic range of the genus. We also included three species of both genera *Adelonema* and *Homalomena* in the ingroup because the relationships between *Adelonema* and the three subgenera of *Philodendron* remained to be resolved (Gauthier et al., 2008; Wong et al., 2013, 2016). Within *Philodendron*, we sampled 125 taxa (137 accessions), which represent all accepted subgenera and sections within subgenus *Philodendron*, including the type of the genus (Krause, 1913; Mayo, 1988, 1989, 1991; Grayum, 1996; Croat, 1997; Köster and Croat, 2011). Based on phylogenetic analyses of the entire Araceae (Cusimano et al., 2011; Nauheimer et al., 2012), we selected 11 taxa from 10 aroid genera as outgroups, including species from the subfamilies Pothoideae (*Anthurium hookeri* Kunth and *Anthurium scandens* [Aubl.] Engl.), Monsteroideae (*Spathiphyllum blandum* Schott), Lasioideae (*Urospatha sagittifolia* [Rudge] Schott), and Aroideae (*Aglaonema marantifolium* Blume, *Anchomanes difformis* [Blume] Engl., *Colocasia esculenta* [L.] Schott, *Montrichardia linifera* [Arruda] Schott, *Pseudohydrosme gabunensis* Engl., *Schismatoglottis calyptrata* [Roxb.] Zoll. & Moritzi, and *Zantedeschia rehmannii* Engl.) (Appendix S1, see Supplemental Data with this article).

Genomic DNA was extracted from silica-dried leaf tissues using the CTAB method of Doyle and Doyle (1987), with extraction of three fractions for each sample (Borsch et al., 2003). DNA stocks were kept at −20°C, and usually 1:10 working dilutions with water were used for polymerase chain reaction (PCR).

Plastid group II introns of *petD*, *rpl16*, and *trnK*, including the *matK* coding region, were selected on the basis of their utility at both deep and shallow phylogenetic levels in angiosperms (Kelchner, 2002; Borsch and Quandt, 2009). The *petD* region has not yet been used in phylogenetic analyses of *Philodendron*, and only short fragments of the *rpl16* intron (~500 bp) and *trnK/matK* (~450–1600 bp) have been used to date (Gauthier et al., 2008; Loss-Oliveira et al., 2016). The *petD* and *rpl16* regions were amplified and sequenced by adding M13 tails to the amplification primers (Messing, 1983). The *petD* region was amplified and sequenced following Löhne and Borsch (2005), and *rpl16* with primers rpl16F and rpl16R (Campagna and Downie, 1998). The *trnK/matK* region was extended to *psbA* and amplified in two halves using the following primer combinations: trnKF (Wicke and Quandt, 2009) and ARAmatK655R (5′-GGATTCGCATTCGCAAACTACAT-3′; present study), and ARAmatK480F (Hilu et al., 2003) and psbA5'R (Shaw et al., 2005). Instead of primer ARAmatK480F, a further internal specific primer ARAmatK582F (5′-TTCACGAATATCATAATTGG-3′; present study) was designed for *Montrichardia linifera*.

PCR was performed in a peqSTAR Thermocycler 1107D (PeqLab, Erlangen, Germany). The mixture for one reaction for the *rpl16* and *trnK/matK* regions consisted of 10 μL of dNTPs 20 pm/μL, 5 μL of 10x *Taq*-buffer S, 3 μL of $MgCl_2$ with a concentration of 25 mM, 2 μL of each primer with a concentration of 20 pm/μL, 0.3 μL of *Taq* DNA Polymerase with 5 units/μL (PeqLab no. PEQL01-8120, Erlangen, Germany) and 4 μL of DNA template. Ultrapure H_2O was added to obtain the final volume of 50 μL. The PCR mixture for the *petD* region included 4.9 μL of betaine (5M) in addition. Temperature profiles for the PCR amplification of *petD* and *trnK/matK* consisted of an initial denaturation of 1:30 min at 95°C, followed by 34 cycles of 30 s denaturation at 95°C, 1 min of primer annealing at 57°C and 1 min of extension at 72°C, and a final elongation period of 10 min at 72°C. For the *rpl16* region, the temperature profile consisted of an initial denaturation step of 1:30 min at 95°C, followed by 4 cycles of 1 min of primer annealing at 58°C and 1 min of extension at 72°C, 30 cycles of a 30 s denaturation step at 95°C, 1 min of primer annealing at 55°C and 1 min of extension at 72°C, followed by a final extension step at 72°C for 10 min. The PCR products were electrophoresed on 1.5% agarose gels in 1x Tris-acetate-EDTA (TAE) buffer (pH 8.0) and stained with SYBR-Gold (Life Technologies no. S11494, Carlsbad, California, USA). Bands were excised from the gel and cleaned using the GenepHlow

Gel/PCR kit (Geneaid, New Taipei, Taiwan). Cycle sequencing was carried out by Macrogen Europe (Amsterdam, The Netherlands), using either the same primers as in the PCR reactions or M13. DNA samples are deposited at the Botanic Garden and Botanical Museum Berlin (BGBM) and are available via the Global Genome Biodiversity Network (GGBN; Droege et al., 2014).

Sequence files were edited and aligned manually using PhyDE version 0.9971 (Müller et al., 2005). Alignments were generated according to the similarity-based criteria for homology assessment and the motif-alignment principles of Borsch et al. (2003) and Löhne and Borsch (2005). The alignment of *rpl16* sequences was not straightforward due to the occurrence of A/T-rich stem-loop elements. Regions of unclear homology such as many tandem repeats, mononucleotide repeats (microsatellites), and other hypervariable sections were excluded from the final alignment. Indels were coded as binary characters using the simple-indel-coding method (Simmons and Ochoterena, 2000) as implemented in SeqState version 1.4.1 (Müller, 2005). Final DNA sequences were submitted to ENA (www.ebi.ac.uk/ena) with the help of custom Python script (https://github.com/michaelgruenstaeudl/annonex2embl).

Phylogenetic analyses

Parsimony and likelihood analyses were conducted following the recommendations provided by Simmons and Freudenstein (2011). Parsimony analyses were conducted using the "parsimony ratchet" (Nixon, 1999) with PRAP version 2.0b3 (Müller, 2004) in conjunction with PAUP* version 4.0b10 (Swofford, 2003) using the CIPRES portal (Miller et al., 2010). Ratchet settings included 200 iterations, unweighting 25% of the positions randomly (weight = 2), and 100 random addition cycles. A strict consensus tree was constructed from all saved trees. Jack-knife (JK) support was calculated in PAUP by performing a single heuristic search within each 10,000 JK pseudoreplicates using the tree bisection and reconnection (TBR) branch-swapping algorithm and a deletion of 36.79% characters in each replicate and saving 100 trees in each search. Starting trees were generated via stepwise addition with simple sequence addition.

The likelihood scores of potential models of sequence evolution for each partition and for the combined dataset were evaluated using jModelTest version 2.1.7 (Darriba et al., 2012). We selected the best-fitting model under Akaike's Information Criterion (AIC). For the initial tree search, the improved version of the neighbor-joining algorithm BIONJ (Saitou and Nei, 1987) was used (Gascuel, 1997).

The maximum likelihood tree was estimated using the graphical user interface (GUI) of RAxML version 1.5b1 (Silvestro and Michalak, 2012). Rapid bootstrap support (BS) was estimated based on the majority-rule consensus tree from 1000 pseudoreplicates with 200 searches. The general time-reversible (GTR) + Γ and the binary (BIN) + Γ models were used for the nucleotide partition and indel partition, respectively.

The nucleotide data were partitioned for Bayesian inference as follows: (1) *petD*: three partitions (*petB* spacer with TVM + I, *petD* 5′ exon with F81, and *petD* intron with TPM1uf + Γ), (2) *rpl16*: one partition (*rpl16* intron with TIM2 + Γ), and (3) *trnK/matK*: 4 partitions (*matK* with TVM + I + Γ, *trnK* 3′ exon with JC, *trnK* 3′ intron with TVM + I, and *trnK* 5′ intron with TPM1uf + Γ). The corresponding indel matrices were added using the restriction site (binary) model (F81-like model) as recommended by Ronquist et al. (2011) for gaps and other binary characters. Bayesian inference analyses were conducted in MrBayes version 3.2 (Ronquist and Huelsenbeck, 2003) on CIPRES. Four runs each with four chains were performed for 50 million generations, sampling every 10,000 generations. Results were processed in Tracer version 1.6.0 (Bouckaert et al., 2014) to check for convergence. The first 10% of trees were discarded as burn-in; the remaining trees were used to construct a 50% majority-rule consensus tree.

The 50% mayority-rule consensus tree obtained in MrBayes was processed in TreeGraph version 2.13.0-748 beta (Stöver and Müller, 2010). Support values obtained in maximum parsimony and maximum likelihood analyses were added with the function "Add support values" in TreeGraph. Simultaneously, this function allows the detection of conflicts between nodes and branches obtained in the MrBayes tree and the maximum parsimony and maximum likelihood. The final PDF file was edited using the open source vector graphics editor Inkscape version 0.92 (The Inkscape Project, http://inkscape.org).

Divergence-time estimates

Testing of the optimal speciation tree prior for divergence-time estimates in *Philodendron* were conducted in BEAST version 1.8.2 (Xie et al., 2011). As a prior of the clock model (strict vs. uncorrelated lognormal relaxed clock [UCLN]; Drummond et al., 2006), we selected the UCLN. This model with a distinct rate along branches drawn from a lognormal distribution is considered more robust to avoid violation of assumptions about clock rate variation and has a better fit to simulated empirical datasets than the strict or autocorrelated clock models (Crisp et al., 2014). Furthermore, in the UCLN analyses, a coefficient of variation higher than zero (>0.5) was obtained, which confirmed that the data did not fit a clock-like model (Drummond and Bouckaert, 2015). In order to select the appropriate branching process (speciation tree) prior to be used in subsequent divergence-time analyses, we conducted a marginal likelihood estimation (MLE) using stepping-stone sampling (SSS) with 150 path steps in BEAST (Xie et al., 2011). The choice of branching process prior has been shown to bias node-age estimates (Condamine et al., 2015) and therefore we tested its effect under both birth-death and Yule speciation models separately. Each analysis was set with a chain length of 1 million iterations and using a simple model with two partitions: (1) the combined nucleotide and (2) the indel matrix under the GTR – Γ and the multistate stochastic Dollo model (Alekseyenko et al., 2008; Woodhams et al., 2013), respectively. Other parameters were set by default in the GUI application for generating BEAST XML files (BEAUTi). The MLE values were used to calculate log-Bayes factors (BFs); BF values >5 indicated that one model was significantly favored over the other (Baele and Lemey, 2013). Based on the results of the MLE using the SSS analyses and BFs, the birth-death speciation prior best fit the data (139.93; Table 1). Therefore, all final analyses were conducted using a birth-death speciation prior under a UCLN.

TABLE 1. Values of the marginal likelihood estimation and Bayes factor analyses using stepping-stone sampling with 150 path steps.

Speciation prior (under UCLN)	ESS	MLE	BF
Birth-death model	>200	−25693.48	139, 93
Yule model	>200	−25833.41	

Notes: UCLN = uncorrelated lognormal model, ESS = effective sample size, MLE = marginal likelihood estimation, BF = Bayes factor.

Divergence-time estimates in* Philodendron*: Calibration approaches—Molecular dating was performed in BEAST version 2.4.3 (Bouckaert et al., 2014), using the corresponding version of BEAUTi to set the parameters. We assessed two calibration approaches (Table 2): one consisted of three secondary constraints, and the other consisted of a fossil in combination with a secondary constraint (fossil+secondary constraint; Table 2). Here, we refer to a secondary calibration point as a divergence-time estimation that was derived from a molecular dataset on the basis of a primary external calibration point, usually one based on paleontological considerations (Shaul and Graur, 2002). The data partitions and substitution models were set according to jModelTest (*matK* = TVM + I +Γ, *petB* spacer and *trnK* 3′ intron = TVM + I, *petD* 5′ exon = F81, *petD* intron and *trnK* 5′ intron = TPM1uf + Γ, *trnK* 3′ exon = JC and *rpl16* intron = TIM2 + Γ). For all substitution models, rates of transitions were set in the XML file according to AIC values of jModelTest. For indels, we applied the multistate stochastic Dollo model.

Node selection for the secondary calibration and the fossil+secondary calibration approaches—The use of secondary calibrations is the only source of calibration information for many groups, particularly for those in which the fossil record is scarce or nonexistent, such as epiphytes in the wet tropics (Forest, 2009; Hipsley and Müller, 2014). To supplement secondary calibrations in studies of lineages where the focal group has no fossils, one option is to sample more distantly related clades that include paleontological records (Schenk, 2016). To date, no fossil has been attributed to *Philodendron* or its closely related genera (Mayo, 1991; Croat, 1997; Mayo et al., 1997; Loss-Oliveira et al., 2016). There is, however, one reliable fossil attributed to the Neotropical genus *Montrichardia* (Herrera et al., 2008) that is, like *Philodendron*, nested within subfamily Aroideae (Cusimano et al., 2011; Nauheimer et al., 2012). Previous phylogenetic studies including a broad taxon sampling across Araceae were conducted applying fossil calibration points, but these included only one species of *Philodendron* (Nauheimer et al., 2012). Our goal was, therefore, to test two calibration strategies: (1) secondary calibration and (2) fossil+secondary calibration.

We sampled as broadly as possible to include nodes strongly supported in the divergence-time analyses based on multiple fossil calibrations across the family Araceae by Nauheimer et al. (2012); nodes 28, 109, and 113 in Nauheimer et al. (2012) all received PP = 1.0. Thus, the following nodes correspond to those suitable for secondary calibration constraints given our taxon sampling: starting with the crown age of the *Philodendron* clade in Nauheimer et al. (2012; node 113) that includes the genera *Adelonema*, *Furtadoa*, *Homalomena*, and *Philodendron* according to Cusimano et al. (2011). A second constraint (node 109) corresponded to the crown age of one of the major lineages within the subfamily Aroideae represented in our study by *Anchomanes difformis* and *Pseudohydrosme gabunensis* from Nephthytideae, *Aglaonema marantifolium* from Aglaonemateae, and *Zantedeschia rehmannii* from the *Zantedeschia* clade and the *Philodendron* clade. To calibrate the root of our tree, we used the crown age of the split of the subfamilies Aroideae+Zamioculcadoideae and Lasioideae from Nauheimer et al. (2012; node 28). In order to incorporate a fossil calibration, we included the species *Montrichardia linifera* (Herrera et al., 2008) and two representatives of its closely related lineages (*Colocasia esculenta* and *Schismatoglottis calyptrata*) according to Nauheimer et al. (2012).

TABLE 2. Parameters used in the secondary and fossil+secondary calibration approaches. Upper and lower values used are depicted in millions of years.

Node	UCLN (secondary calibration)	UCLN (fossil+secondary calibration)
28*	80–100 Ma; U	NA
109*	54–81 Ma; U	NA
113*	11–39 Ma; U	11–39 Ma; U
Fossil (*Montrichardia aquatica*)	NA	Mean = 58.7 Ma (61.7–55.8 Ma); E

Notes: UCLN = uncorrelated lognormal model, U = uniform prior, E = exponential prior, NA = not applicable, and asterisks denote nodes by Nauheimer et al. (2012).

Parameters used in the secondary and fossil+secondary calibration approaches—In the secondary calibration approach, the three nodes were constrained under a uniform distribution prior (Table 2). This distribution is recommended for such calibrations, allowing every age between the upper and lower bounds to have equal prior probability (Schenk, 2016). We applied the mean and 95% HPD intervals obtained by Nauheimer et al. (2012) in the BEAST analysis under a UCLN model with a uniform prior and a Jukes-Cantor (JC) + Γ tree model. The following initial and upper values were applied: 80 Ma and 100 Ma (node 28), 54 Ma and 81 Ma (node 109), and 11 Ma and 39 Ma (node 113).

In the fossil+secondary calibration approach, two nodes were constrained (Table 2). The first node was constrained using the minimum age of a fossilized leaf identified as *Montrichardia aquatica* dated from the middle to late Paleocene 61.7–55.8 mya (Herrera et al., 2008). An exponential distribution prior was applied with an offset of 55.8 and a mean of 58.7, constraining the minimum age of the node with this fossil (*Colocasia esculenta*, *Montrichardia linifera*, and *Schismatoglottis calyptrata*). The mean value of 58.7 was selected based on the mean age estimated for the fossil. In an initial study, the fossil constraint had been applied in combination with all three secondary points described above but the nodes calibrated with the ages of nodes 28 and 109 corresponded to the nodes prior and subsequent to the fossil calibrated node, respectively, in the BEAST Maximum clade credibility (MCC) tree topology (Appendix S2). Given the range in calibration ages between these nodes (100 Ma and 81 Ma for the upper values of nodes 28 and 109, respectively) and their proximity to the fossil node, it was not possible to apply a fossil calibration and the entire set of three secondary constraints used in the secondary calibration approach to our dataset. Therefore, we applied the fossil calibration in combination with only one secondary calibration constraint to the ingroup (node 113) as described above (Table 2).

To assess the consistency of the BEAST results, three independent Markov chain Monte Carlo (MCMC) runs were conducted using the same dataset and the same parameters for both secondary and fossil+secondary calibration approaches. Each chain was run for 100 million generations logging parameters every 10,000 generations. Tracer version 1.6.0 (Bouckaert et al., 2014) was used to visualize log files, assess the stationarity on the log-likelihood curves, and determine the burn-in. The first 10% saved trees from each run were discarded, and the remaining trees were combined in Logcombiner version 2.4.3 (Drummond et al., 2012). Treeannotator version 2.4.3 (Bouckaert et al., 2014) was used to estimate the MCC tree with posterior probability values (PP; limit set to 0.5) and mean node ages with the HPD of these ages. MCC trees estimated using different time calibration approaches were then compared in

FigTree version 1.4.2 (Rambaut, 2012) and exported as with the phylogenetic trees described above.

Diversification rate shifts

Heterogeneity in rates of diversification processes (speciation and extinction) and in rate shifts across the genus *Philodendron* was estimated using BAMM version 2.5.0 (Rabosky, 2014; Rabosky et al., 2017). Speciation and extinction might vary through time and among lineages, in particular in clades such as *Philodendron*, where species diversity is imbalanced among subgenera. BAMM detects these rate shifts without a priori hypotheses on the number and location of these events based on a birth-death process. The MCC trees from the BEAST analyses with both secondary calibration and fossil+secondary calibration approach were used as input files without outgroup. The priors for the diversification rate analyses were set using the "setBAMMPriors" command in the "BAMMtools" package version 2.1.6 (Rabosky et al., 2014) in R version 1.1.419 (R Core Team, 2013). Incomplete taxon sampling can bias inferences of diversification rates (Shi and Rabosky, 2015). We therefore specified the fraction of missing species in each subgenus of *Philodendron* under the assumption of random taxon sampling (FitzJohn et al., 2009). The sampling fraction was calculated as a ratio of the number of species included divided by the total number of species currently accepted: *Meconostigma*: 3/21, *Pteromischum*: 8/82, and *Philodendron* 119 (126 accessions)/457, these proportions were used as inputs for the "SamplesProbsFilename" argument in the Control File. To test the sensitivity of the sampling fraction, we set two additional analyses for the MCC tree from the BEAST analysis with secondary calibrations where we assumed one smaller sampling fraction for each subgenus (0.05) and another with a larger one (0.5) (see also Shi and Rabosky, 2015). Given the ongoing debate on the theoretical foundations of the inference model in BAMM (Moore et al., 2016; Rabosky et al., 2017), we used the "BAMMlikelihood" function as recommended by Rabosky et al. (2017), which returns the log-likelihood for a given configuration of events on a phylogenetic tree. We used the same priors for the sampled fraction analysis and obtained a similar value for the log-likelihood of the final generation. According to Rabosky et al. (2017), similar or identical values indicate that BAMM is correctly computing the likelihood. These analyses were conducted using a Poisson prior value of 1.0 for the "ExpectedNumberofShifts" as recommended by Rabosky et al. (2014) and Shi and Rabosky (2015) that is more conservative and implies a null hypothesis of zero rate shifts across the phylogeny. BAMM was implemented in the C++ command line. We ran four parallel MCMCs for 50 million generations and sampled the results every 5000 generations. The output files were analyzed in R, using the "BAMMtools" package.

Convergence was assessed in the R package "coda" (Plummer et al., 2006) by checking the ESS values for likelihood and number of shift events, the first 10% of the sampled generations were discarded as burn-in. Values >200 were considered indicative of convergence. Bayes factors were computed to compare the evidence for models with at least one rate shift to the evidence for the null model using the "computeBayesFactors" function. The event output files were analyzed by discarding 10% burn-in samples and assessing the distinct rate shift configurations within the 95% credible set using the "credibleShiftSet" function. Subsequently, the position(s) of the significant rate shift was inferred by observing the nodes with the highest PP values (up to 95%) using the "distinctShiftConfigurations" function. To complement our analyses, we estimated rate shifts through time using the "credibleShiftSet" function. A burn-in of 10% was applied and a diversification rate plot through time was obtained using the "plotRateThroughTime" function. This analysis was carried out initially for the entire dataset and, in order to visualize separately the diversification process for the subgenera, we plotted two datasets separately: the clade corresponding to the subgenera *Meconostigma* and *Pteromischum* and the clade corresponding to subgenus *Philodendron*.

RESULTS

Phylogenetic analyses

Individual matrices contained 154 new sequences for the *petD*, *rpl16*, and *trnK/matK* regions and 1259, 2898, and 3197 aligned nucleotides, respectively. In cases of intraspecific variation in one, two, or three plastid regions, multiple sequences for the same species were maintained in the alignment. After excluding hotspots in each single-region alignment (*petD*: a poly-A [positions 260–274]; *rpl16*: two poly-A [196–211; 320–330] and two hotspots [765–2029; 2933–2998] and *trnK/matK* three poly-A [249–256; 875–881; 2571–2580], poly-T [2857–2869], and poly-AT [2934–2998]), the combined plastid alignment contained 5204 aligned nucleotides (1107 for *petD*, 1185 for *rpl16*, and 2912 for *trnK/matK*). Simple indel coding resulted in the addition of 267 binary characters (51 for *petD*, 114 for *rpl16*, and 102 for *trnK/matK*; Appendix S3).

Sequence statistics, models of sequence evolution (AIC), and tree statistics for the individual marker alignments and the combined plastid dataset are presented in Appendix S4. Bayesian inference, maximum likelihood, and maximum parsimony analyses of the combined plastid dataset produced nearly identical topologies with the exception of two inconsistent placements of the species *Colocasia esculenta*, *Montrichardia linifera*, *Schismatoglottis calyptrata*, and *Zantedeschia rehmannii* and inconsistences found within the subgenus *Philodendron* (clades 5–14) (displayed in square brackets in Fig. 2).

***Phylogenetic relationships between the genera* Adelonema, Homalomena, *and* Philodendron**—The MrBayes 50% majority-rule consensus tree based on the analysis of the combined plastid dataset with node support values for maximum likelihood, maximum parsimony, and Bayesian inference is shown in Fig. 2. *Homalomena* is supported as monophyletic (BS = 100, JK = 100, PP = 1.0) and resolved as sister to a clade consisting of the Neotropical genera *Adelonema* and *Philodendron* (BS = 83, JK = 85, PP = 0.83). The genera *Adelonema* and *Philodendron* are both resolved as monophyletic groups (BS = 91, JK = 96, PP = 1.0 and BS = 94, JK = 92, PP = 1.0, respectively).

***Relationships within the genus* Philodendron**—Within *Philodendron*, two major lineages are found (lineages A and B; Fig. 2). Lineage A (BS = 90, JK = 94, PP = 0.92) contains the subgenera *Meconostigma* (BS = 100, JK = 100, PP = 1.0; clade 1) and *Pteromischum* (BS = 100, JK = 100, PP = 1.0; clade 2), and lineage B (BS = 100, JK = 100, PP = 1.0) corresponds to the larger subgenus *Philodendron*. Within subgenus *Philodendron*, there are 12 well-supported clades (clades 3–14; Fig. 2). The first clade (clade

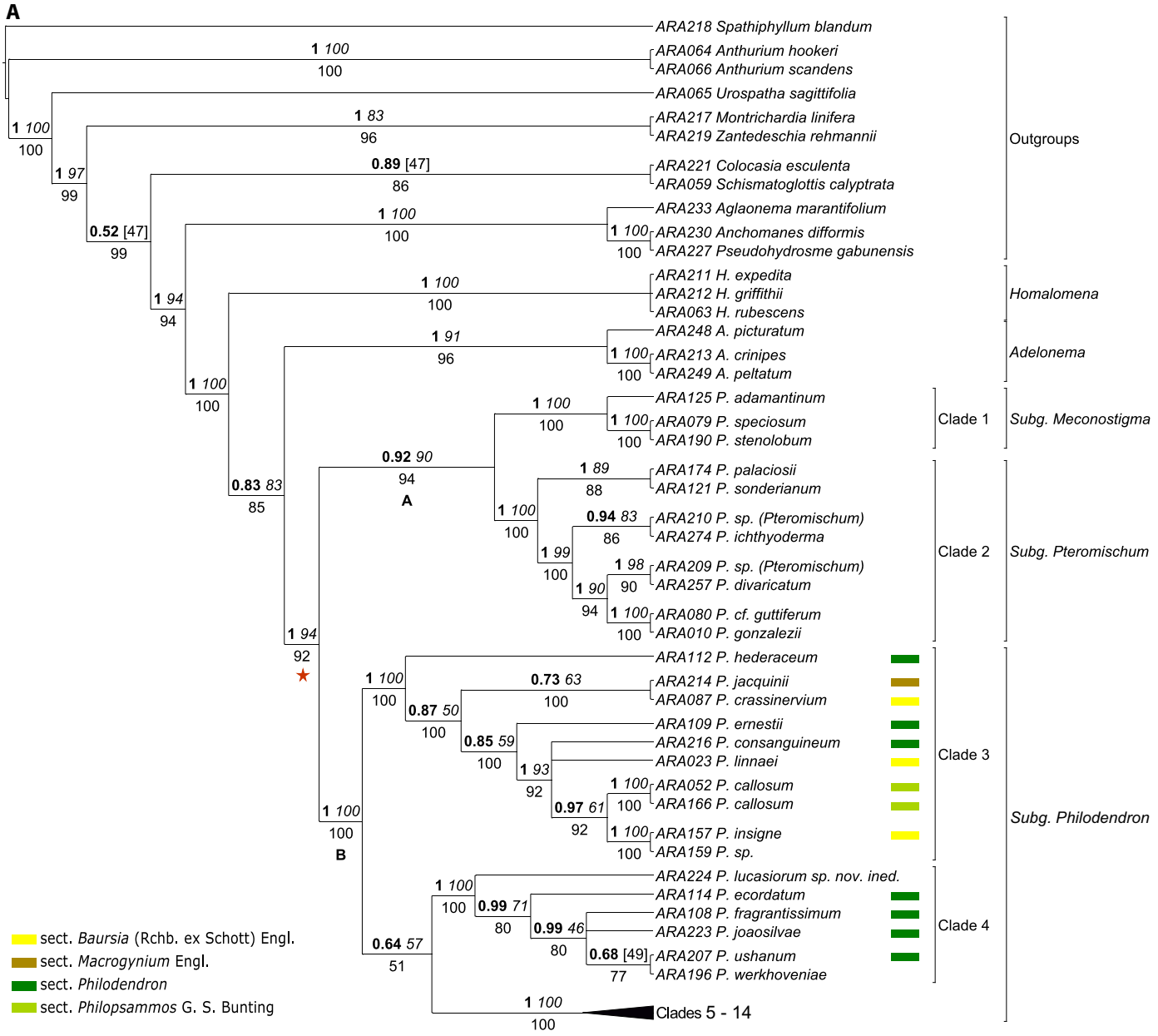

FIGURE 2. (A-C) Bayesian 50% majority-rule consensus tree of *Philodendron* with three plastid markers (*petD*, *rpl16*, and *trnK/matK*). Values above nodes indicate posterior probability (bold) and bootstrap (italic) support, and values below nodes indicate jack-knife support. Values in square brackets indicate conflicting topologies between Bayesian inference and maximum likelihood (above branches) and maximum parsimony (below branches) detected in TreeGraph. Node tips correspond to DNA number and species names (see Appendix S1 for specimen details). Red star = genus *Philodendron*; A = subgenera *Meconostigma* + *Pteromischum*; B = subgenus *Philodendron*. Key, bottom left: sections recognized within subgenus *Philodendron* (Croat, 1997; Croat and Köster, 2011). Colored boxes next to tips indicate the sectional attribution, which is unknown or ambiguous for species without boxes. [Correction added on July 26, 2018 after first online publication: In a previous version of this article, Figure 2A contained a technical error in which the figure part label obstructed part of the figure information. This has been corrected.]

3) consists of species from different geographic regions of the Neotropics, including *P. hederaceum* (Jacq.) Schott, the most widespread *Philodendron* species, which essentially covers the entire range of the genus. The next branching clade (clade 4) comprises species endemic to the Guianas, with the single exception of the very widespread species *P. fragrantissimum* (Hook.) G. Don. Clades 5–14 form the highly supported core of subgenus *Philodendron* (BS = 100, JK = 100, PP = 1.0; Fig. 2).

Divergence-time estimates in the secondary calibration approach

The BEAST tree based on the secondary calibration approach is presented in Fig. 3 with crown and stem node age estimates for the clades proposed in Table 3. Stem ages of ~111.14 Ma (95% HPD: 81.75–148.17) for the clade consisting of subfamilies Pothoideae and Monsteroideae and of ~87.74 Ma (95% HPD: 80.1–97.51) for the clade

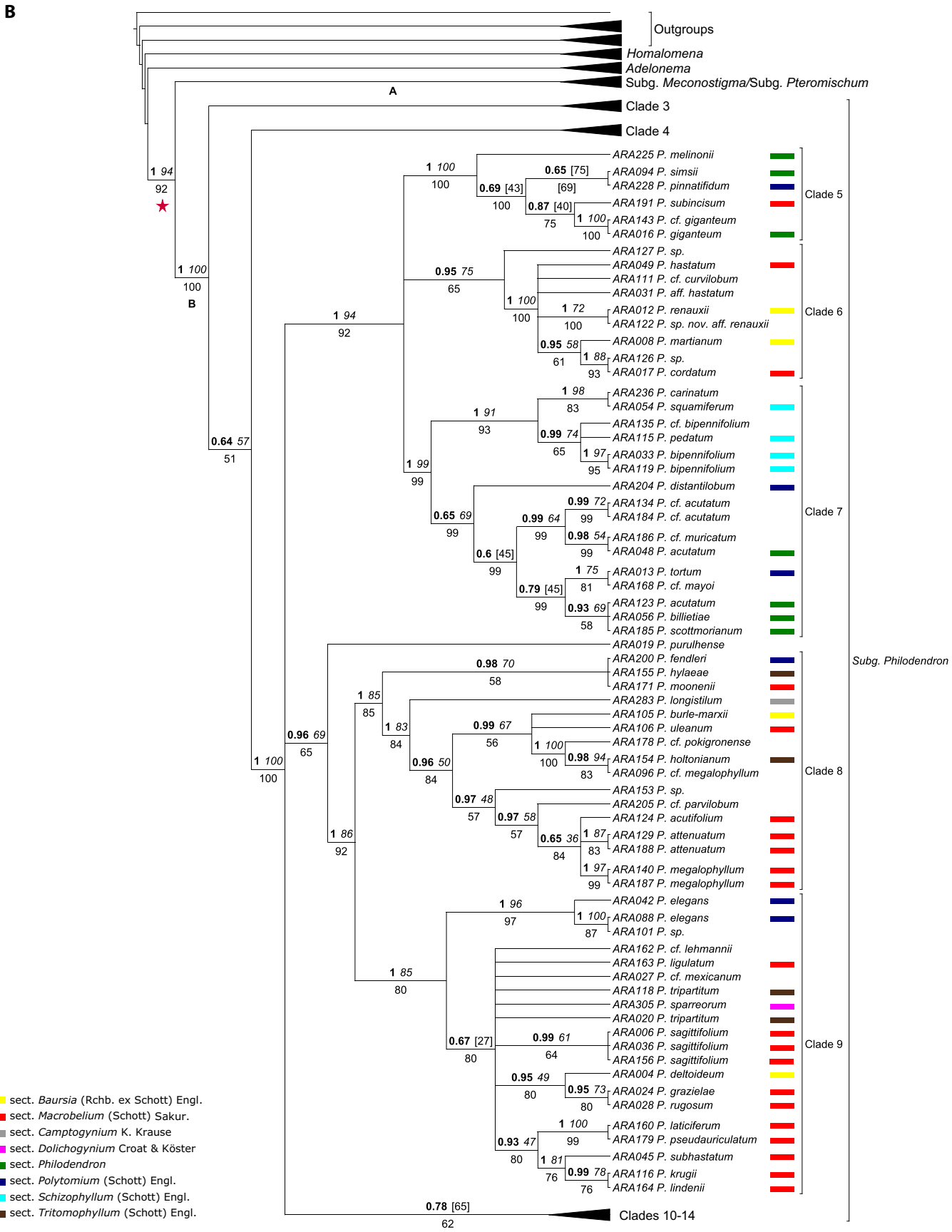

FIGURE 2. (continued)

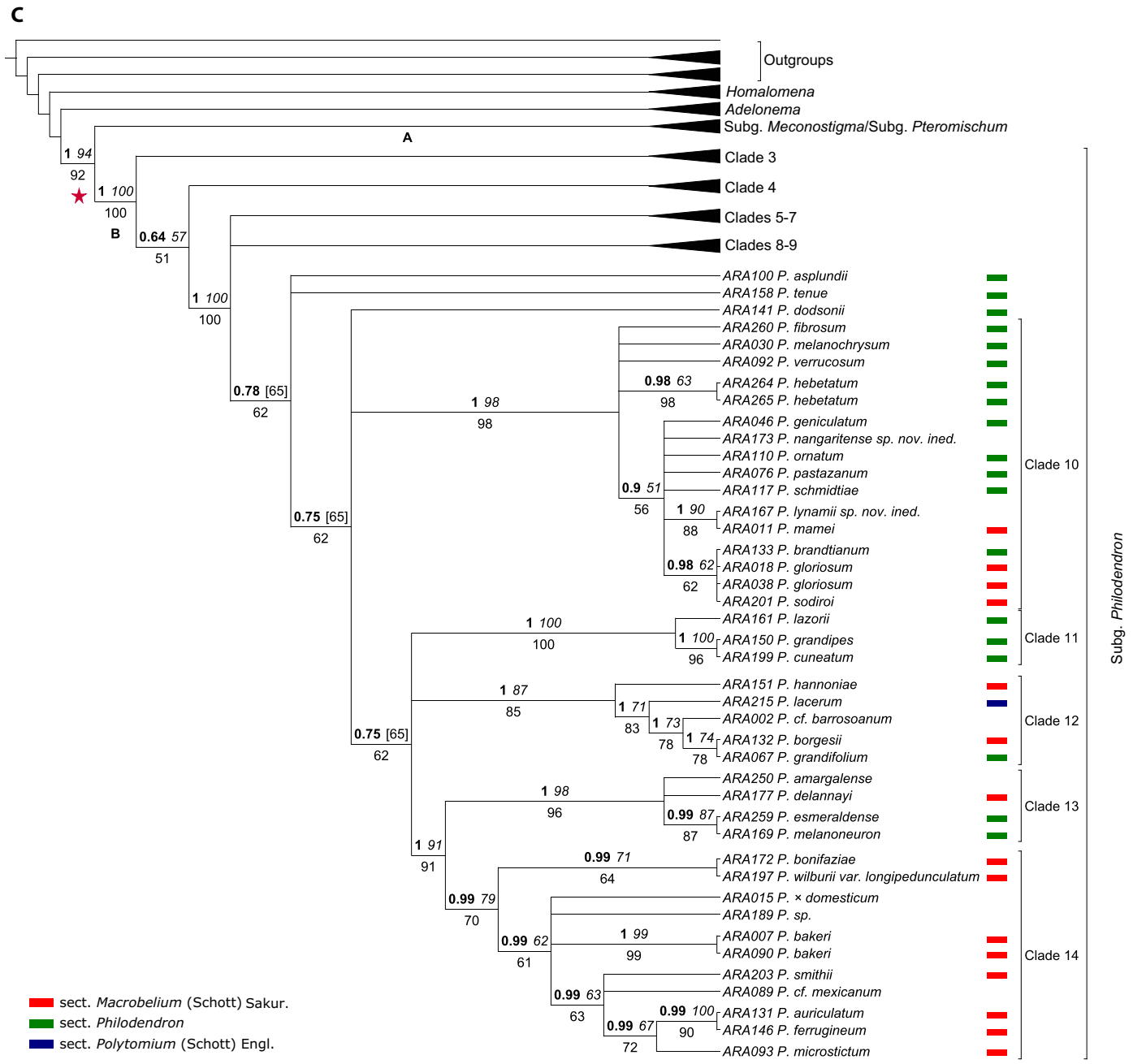

FIGURE 2. (continued)

including subfamilies Lasioideae and Aroideae+Zamioculcadoideae were estimated. The stem age of the ingroup containing *Homalomena*, *Adelonema*, and *Philodendron* was estimated ~53.28 Ma (95% HPD: 39.18–66.23). The stem age of the clade containing *Adelonema* and *Philodendron* was inferred to be ~27.31 Ma (95% HPD: 18.9–36.64). The diversification of *Philodendron* and *Adelonema* occurred ~25.53 mya (95% HPD: 17.81–33.94), in the late Oligocene.

Within genus *Philodendron*, the split between subgenus *Philodendron* and the clade consisting of subgenera *Meconostigma* and *Pteromischum* was estimated as ~22.1 mya (95% HPD: 15.48–29.79) in the early Miocene. The crown nodes of the subgenera *Meconostigma*, *Pteromischum*, and *Philodendron* were estimated to be ~6.66 Ma (95% HPD: 2.55–11.88), ~14.56 Ma (95% HPD: 8.64–20.54), and ~18.06 Ma (95% HPD: 12.3–24.44), respectively. Within subgenus *Philodendron*, in contrast to Bayesian inference, maximum likelihood, and maximum parsimony trees, clade 12 was recovered as sister to a major clade containing clades 5–14 in the BEAST analyses (Figs. 2 and 3; Appendix S2). Clades 5, 6, and 11 were not supported. The remaining clades within subgenus *Philodendron* diversified during the past 11 Ma (Fig. 3 and crown ages in Table 3).

Divergence-time estimates in the fossil+secondary calibration approach

Inferences with the fossil+secondary calibration approach resulted in overall younger ages compared to the ages inferred with

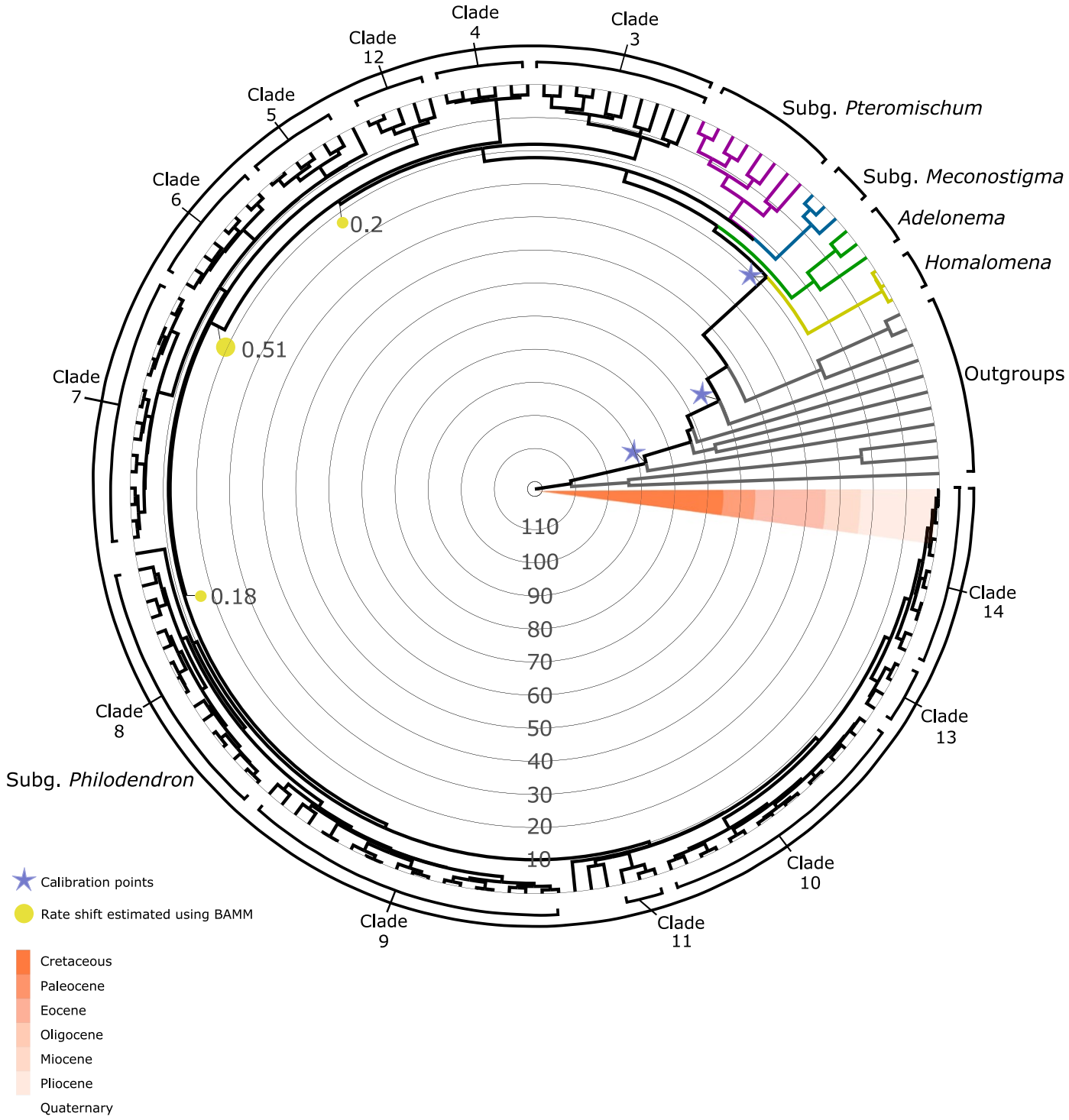

FIGURE 3. Maximum clade credibility (MCC) chronogram obtained in BEAST based on three plastid markers (*petD*, *rpl16*, and *trnK/matK*) with age estimates with three secondary calibration constraints. Time intervals in millions of years ago are indicated by black circles. Geologic time scale is indicated by the orange gradient band. Violet stars correspond to secondary calibration points to specific nodes referred to in the text. Yellow circles correspond to three posterior distributions of the diversification rate shift estimated with BAMM. Refer to Table 3 for details of percent HPD values for divergence-time estimates.

the secondary calibration approach (Table 3; Appendices S2, S5). The stem age of the node consisting of subfamilies Pothoideae and Monsteroideae was estimated to be ~87.1 Ma (95% HPD: 57.14–121.31); the stem age of subfamilies Lasioideae and Aroideae+Zamioculcadoideae was estimated to be ~72.91 Ma (95% HPD: 59.24–87.46). The stem age of the ingroup containing

TABLE 3. Branch supports and divergence-time estimates (Ma) using BEAST under birth-death speciation prior.

		Secondary constraint approach			Fossil+secondary constraint approach			Divergence-time estimates obtained by Nauheimer et al. (2012): UCLN model with a uniform prior and a Jukes-Cantor + Γ tree model	
Clade	**Node**	**BEAST-PP**	**Mean**	**HPD**	**BEAST-PP**	**Mean**	**HPD**	**Mean**	**HPD**
Pothoideae + Monsteroideae	S	1.00	1111.14	81.75–148.17	1.00	87.1	57.14–121.31	96.73	86.62–107.06
	C	0.75	93.81	46.03–121.14	0.82	68.46	29.48–95.05	81.06	68.3–93.68
Lasioideae (secondary constraint approach)	S	1.00	87.74	80.1–97.51	0.68	72.91	59.24–87.46	90.23 (node 28)	80.09–100.68
	C	NA (Single terminal node)			NA (Single terminal node)				
Aroideae	S	1.00	87.74	80.1–97.51	0.68	72.91	59.24–87.46	86.95	77.1–97.03
	C	1.00	72.99	59.64–83.53	0.95	60.91	55.89–67.77	82.12	73.24–92.28
Anchomanes difformis, *Pseudohydrosme gabunensis*, *Aglaonema marantifolium*, and *Zantedeschia rehmannii* + *Philodendron* clade (secondary constraint approach)	S	1.00	71.21	59.39–81.49	0.98	51.82	39.88–62.63	68.17 (node 109)	54.06–81
	C	1.00	60.51	47.07–73.78	0.97	45.23	32.84–56.95	40.69	24.48–57.71
Montrichardia (fossil+secondary constraint approach)	S	1.00	72.99	59.64–83.53	1.00	57.6	55.8–61.22	Not supported	
	C	1.00	66.25	50.11–81.07	0.99	52.16	40.58–60.64	NS	
Philodendron clade (both approaches)	S	0.96	53.28	39.18–66.23	0.97	45.23	32.84–56.95	NS	
	C	1.00	27.31	18.9–36.64	1.00	23	15.01–32.53	25 (node 113)	11.88–39.4
Homalomena	S	1.00	27.31	18.9–36.64	1.00	23	15.01–32.53	NS	
	C	1.00	1.41	0.2–3.12	1.00	1.2	0.17–2.7	NS	
Adelonema	S	0.79	25.53	17.81–33.94	0.76	21.55	13.87–29.89	NS	
	C	1.00	17.05	8.76–26.26	1.00	14.23	6.91–22.39	NS	
Philodendron	S	0.79	25.53	17.81–33.94	0.76	21.55	13.87–29.89	NS	
	C	1.00	22.1	15.48–29.79	1.00	18.61	12.19–26.12	NS	
Subgenus *Meconostigma*	S	0.37	21.69	*	1.00	18.61	12.19–26.12	NS	
	C	1.00	6.66	2.55–11.88	1.00	5.61	1.94–9.98	NS	
Subgenus *Pteromischum*	S	0.37	21.69	*	0.37	18.32	*	NS	
	C	1.00	14.56	8.64–20.54	1.00	12.22	7.11–18.05	NS	
Subgenus *Philodendron*	S	1.00	22.1	15.48–29.79	0.37	18.32	*	NS	
	C	1.00	18.06	12.3–24.44	1.00	15.19	9.64–21.26	NS	
Clade 3	S	1.00	18.06	12.3–24.44	1.00	15.19	9.64–21.26	NS	
	C	1.00	11.1	6.85–15.63	1.00	9.34	5.34–13.6	NS	
Clade 4	S	0.85	16.91	11.2–22.65	0.85	14.21	8.9–19.87	NS	
	C	1.00	3.93	1.75–6.66	1.00	3.28	1.39–5.66	NS	
Clade 5	S	0.18	8.8	*	0.17	7.6	*	NS	
	C	0.18	5.15	*	1.00	4.34	2.21–6.81	NS	
Clade 6	S	0.18	9.03	*	0.17	7.6	*	NS	
	C	1.00	4.33	2.21–6.81	0.25	7.25	*	NS	
Clade 7	S	1.00	9.13	5.81–12.85	1.00	7.7	4.63–11.22	NS	
	C	1.00	4.69	2.56–7.09	1.00	3.95	2.05–6.21	NS	
Clade 8	S	0.96	7.87	4.95–11.01	0.96	6.64	4.03–9.61	NS	
	C	1.00	6.25	3.76–8.95	1.00	5.27	3.04–7.76	NS	
Clade 9	S	0.96	7.87	4.95–11.01	0.96	6.64	4.03–9.61	NS	
	C	1.00	6.08	3.59–8.82	1.00	5.12	2.91–7.7	NS	
Clade 10	S	0.76	7.46	4.56–10.47	0.74	6.3	3.69–9.02	NS	
	C	1.00	4.08	2.15–6.16	1.00	3.44	1.78–5.35	NS	
Clade 11	S	0.17	8.65	*	0.96	7.65	4.77–11	NS	
	C	0.18	4.1	*	1.00	3.44	1.48–5.84	NS	
Clade 12	S	1.00	12.03	7.87–16.37	0.23	9.98	*	NS	
	C	1.00	6.97	3.13–11.01	1.00	5.81	2.98–9.47	NS	
Clade 13	S	1.00	5.71	3.24–8.34	1.00	4.81	2.65–7.23	NS	
	C	1.00	3.35	1.58–5.43	1.00	2.8	1.24–4.59	NS	
Clade 14	S	1.00	5.71	3.24–8.34	1.00	4.81	2.65–7.23	NS	
	C	1.00	4.1	2.1–6.39	1.00	3.45	1.69–5.48	NS	

Notes: UCLN = uncorrelated lognormal model, C = crown node, S = stem node, PP = posterior probability, HPD = 95% intervals, asterisk = calculated given the low statistic support, NA = not applicable, and NS = not sampled in Nauheimer et al. (2012). Names between brackets in the first column indicate nodes calibrated in each approach.

Homalomena, *Adelonema*, and *Philodendron* was estimated at ~45.23 Ma (95% HPD: 32.84–56.95). The stem age of the clade containing *Adelonema* and *Philodendron* was inferred to be ~21.55 Ma (95% HPD: 13.87–29.89). The diversification of *Philodendron* and *Adelonema* occurred ~18.61 mya (95% HPD: 12.19–26.12), in the early Miocene.

The topology of the BEAST analysis based on the fossil+secondary calibration approach differs from that of the BEAST tree based on the secondary calibration approach in resolving subgenus *Meconostigma* as sister to a clade consisting of the subgenera *Philodendron* and *Pteromischum* (Appendix S2). The split between subgenus *Meconostigma* and the clade containing subgenera *Philodendron* and *Pteromischum* was estimated to be ~18.61 Ma (95% HPD: 12.19–26.12). Within subgenus *Philodendron*, the nodes of clades 5, 6, and 12 were not supported.

Diversification rate shifts

The likelihood of the BAMM MCMC reached convergence, and the post-burn-in ESS values were >200 for rate shift analyses of both the fossil+secondary and the secondary calibration approaches (Appendix S6). A model with one shift received a higher BF in comparison to the models with zero, two, three, and four shifts for trees of both calibration approaches (Table 4). Different values used for the sampling fractions in the BAMM analyses showed no effect on the number of evolutionary shifts or on the estimation of speciation and extinction rates. BAMM results of the 95% credible set of shift configurations under the three sampling-fraction assumptions identified a diversification rate shift within subgenus *Philodendron* (Appendix S7). According to the analysis accounting for the random taxon sampling (Appendix S7), three of the four configurations within the 95% credible set (posterior distributions = 0.51, 0.18, and 0.2) showed a rate shift occurring near the base of subgenus *Philodendron*. The shift with 0.2 posterior distribution occurred on the branch prior to the divergence of clades 4–14, the shift with the highest posterior distribution (0.51) was located on the branch prior to the divergence of clades 5–14, and the shift with 0.18 posterior distribution was located on the branch prior to the divergence of clades 5–14 (excluding clade 12) (Fig. 3; Appendix S7). In Figure 4, the blue line corresponds to the diversification process of subgenus *Philodendron* beginning ~18 mya, whereas the dark green line corresponds to the diversification process of the lineage including the subgenera *Meconostigma* and *Pteromischum* beginning ~21 mya. The diversification process of the two lineages began with a similar speciation rate (~0.30 events/Ma/lineage); subsequently (by ~12 mya), the speciation rate of subgenus *Philodendron* had increased to ~0.55 events/Ma/lineage, whereas the diversification of the lineage containing the subgenera *Meconostigma* and *Pteromischum* remained ~0.30 events/Ma/lineage. The diversification rate of subgenus *Philodendron* dropped slightly at ~10 mya to 0.48 events/Ma/lineage, followed by another increase to ~0.58 events/Ma/lineage at ~8.5 mya; from that time to the present day, the diversification rate has continued to increase. The current diversification rate of subgenus *Philodendron* was estimated to be ~0.73 events/Ma/lineage, whereas the diversification rate of the subgenera *Meconostigma* and *Pteromischum* remained relatively stable and increased by ~0.05 events/Ma/lineage to ~0.35 events/Ma/lineage.

TABLE 4. Bayes factor (BF) comparison of the models with posterior or prior greater than zero under the two calibration approaches.

Calibration approach	Expected number of shifts	BF
Fossil+secondary calibration	0	1.0
	1	33.11
	2	8.88
	3	1.42
	4	1.06
Secondary calibration	0	1.0
	1	14.46
	2	2.98
	3	0.88
	4	0.16

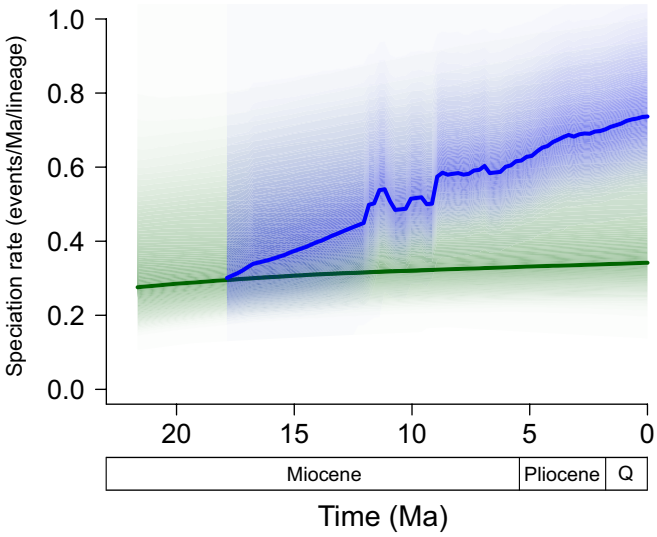

FIGURE 4. *Philodendron* speciation rate through time (events/Ma/lineage) according to BAMM analysis using the MCC calibrated with three secondary constraints. Color density shading area indicates 95% Bayesian credible region of the distribution of rates. Blue line corresponds to the speciation rate of subgenus *Philodendron*. Dark green line corresponds to the speciation rate of the subgenera *Meconostigma* and *Pteromischum*. Abbreviation: Q = Quaternary.

DISCUSSION

Phylogenetic relationships between the genera *Adelonema*, *Homalomena*, and *Philodendron*

In the present study, the Asian genus *Homalomena* is resolved as sister group to a clade including the Neotropical genera *Adelonema* and *Philodendron* (Figs. 2 and 3). This result is congruent with the maximum parsimony trees based on nuclear DNA data (ETS and ITS with 48 and 31 species of *Philodendron*, respectively) obtained by Gauthier et al. (2008) and the topologies obtained by Wong et al. (2013) with ITS; by Wong et al. (2016) with ITS and *trnK/matK* partial sequences; and by Loss-Oliveira et al. (2016) with ETS, *trnL-trnF*, and partial *trnK/matK*. Our results support the monophyly of the genera *Adelonema* and *Philodendron*. This result is not congruent with the maximum parsimony tree based on *rpl16* partial sequences with 45 species (Gauthier et al., 2008), the maximum likelihood tree by Wong et al. (2013) based on ITS, or the

Bayesian inference tree by Wong et al. (2016) using ITS and *matK*, which recovered *Philodendron* as a non-monophyletic group with *Philodendron* subgenus *Pteromischum* sister to *Adelonema*. Based on the phylogenetic relationships within *Philodendron*, our results lend support to the taxonomic concept of *Philodendron* subgenus *Pteromischum* as an entity within *Philodendron* (Schott, 1856; Engler, 1899; Krause, 1913; Mayo, 1986; Grayum, 1996). Wong et al. (2013, 2016) documented some morphological similarities supporting a closer phylogenetic relationship between *Adelonema* and subgenus *Pteromischum* (e.g., anisophyllous sympodial growth with several or many leaves per stem article, absent or highly inconspicuous cataphylls, and sheathing petioles). However, apart from the different life forms (species of subgenus *Pteromischum* are vines while *Adelonema* species are strictly terrestrial herbs), floral characters used in the taxonomic circumscription of the genus *Philodendron* (e.g., shape and vascularization patterns in the stamens, style morphology, and number of ovules per locule; Grayum, 1996) as well as certain anatomical characters (e.g., presence of three types of raphide cells; Klimko et al., 2014) are evidence for a closer relationship of *Philodendron* subgenus *Pteromischum* to the other two subgenera of the genus *Philodendron* than to *Adelonema*.

The monophyly of *Philodendron* is strongly supported by our results. Although there is no single morphological feature that unambiguously distinguishes *Philodendron* from closely related genera, the combination of the following characters supports its monophyly: plants usually climbing or epiphytic (if terrestrial herbs, adult plants with conspicuous cataphylls and petiolar sheath much reduced); inflorescences secreting resin at anthesis, either from the adaxial canals of the spathe or from the spadix, rarely from both; spadix with distinct sterile staminate zone between pistillate zone and fertile staminate zone; endothecium nearly always with cell wall thickenings; female flowers without staminodes; ovary with two to many completely separate locules, with axile to basal placentation; and ovules one to many per locule, usually hemiorthotropous, rarely hemianatropous (Grayum, 1996; Croat, 1997; Klimko et al., 2014).

Relationships within the genus *Philodendron*

Analyses of a combination of the *petD*, *rpl16*, and *trnK/matK* regions and the substantially increased sampling (>20% of total species diversity) in the present study provide a more comprehensive hypothesis on the phylogenetic relationships within *Philodendron*, yielding a distinctly higher number of resolved and well-supported clades compared to previous studies (Gauthier et al., 2008; Loss-Oliveira et al., 2016).

The three subgenera of *Philodendron* were recovered as monophyletic groups, although the sister relationship between the subgenera *Meconostigma* and *Pteromischum* is weakly supported (Fig. 2). *Meconostigma* and *Pteromischum* were resolved as monophyletic groups based on ITS and *matK* (Wong et al., 2016) and ETS and ITS (Gauthier et al., 2008). The monophyly of subgenus *Meconostigma* is additionally supported by at least four morphological synapomorphies: a thickened spathe, a well-developed intermediate staminodial zone subequal to longer than staminate portion, the presence of stylar lobes, and an axial vascular system independent of the funicle supply (Braucks Calazans et al., 2014; clade 1; Fig. 2A).

Phylogenetic relationships within subgenus *Philodendron*: Clades recovered and inconsistencies with the current infrageneric classification

Within subgenus *Philodendron*, 12 strongly supported clades are recognized (clades 3–14; Fig. 2). Some of these clades have similar species composition to lineages recognized in the ETS and ITS trees by Gauthier et al. (2008; e.g., *P. ecordatum* Schott and *P. fragrantissimum*, clade 4; *P. melinonii* Brongn. ex Regel and *P. pinnatifidum* (Willd.) Schott, clade 5; and *P. gloriosum* André and *P. ornatum* Schott, clade 10; Fig. 2).

No section from the currently accepted infrageneric classification of subgenus *Philodendron* was recovered as monophyletic, and morphological synapomorphies for the individual clades have not been found. Nevertheless, most of the species with <10 ovules/locule (traditionally attributed to sect. *Macrobelium* [Schott] Sakur. and sect. *Tritomophyllum* [Schott] Engl.) are resolved in two divergent clades: one contains both clades 8 and 9, and the other is clade 14 (Fig. 2). Species with >10 ovules/locule (mostly members of sect. *Philodendron*) are grouped in clades 4, 11, 12, and 13 (Fig. 2). Therefore, this character appears to be homoplastic.

With the exception of clade 3, most of the clades (clades 4–14; Fig. 2) within subgenus *Philodendron* are consistent with geographic patterns rather than with the current taxonomic classification based on morphology. Clades that are geographically defined but inconsistent with the morphological classification have also been documented in *Anthurium* (Carlsen and Croat, 2013), and they are commonly found in recent species-rich Neotropical lineages such as *Costus* L. (Kay et al., 2005) and *Inga* Mill. (Richardson et al., 2001).

Clade 3 (BS = 100, JK = 100, PP = 1.0; Fig. 2A) contains species from different regions (Caribbean, Amazon basin, Guianas, and southeast Brazil), many of which are assigned to sect. *Baursia* (Rchb. ex Schott) Engl. in the current taxonomic classification (Croat, 1997), as well as *P. consanguineum* Schott, *P. ernestii* Engl. and *P. hederaceum*, traditionally attributed to sect. *Philodendron*, and *P. jacquinii* Schott of the monotypic sect. *Macrogynium* (Croat, 1997). Clade 4 (BS = 100, JK = 100, PP = 1.0; Fig. 2A) comprises range-restricted species from the lowland rainforests of the Guianas, with the exception of *P. fragrantissimum*, which occurs from Belize and Cuba through to southeast Brazil. With *P. joaosilvae* Croat, A. Cardoso & Moonen, and *P. werkhoveniae* Croat, this clade includes two terrestrial species among the otherwise appressed-climbing hemiepiphytes or vines.

The remaining clades (5–14; Fig. 2B, C) are organized in three major lineages: clades 5–7; clades 8 and 9; and clades 10–14 and three monospecific branches corresponding to the species *P. asplundii* Croat & M. L. Soares and *P. tenue* K. Koch & Augustin (sisters to clades 10–14) and *P. dodsonii* Croat & Grayum (sister to clade 10). Clade 5 (BS = 100, JK = 100, PP = 1.0) includes epiphytic species from South America and the Caribbean, with the exception of *P. subincisum* Schott, a species endemic to northern Veracruz in Mexico (Croat, 1997). All species of clade 5 have persistent cataphylls decaying as fibers, a character state that has been used in combination with others for the circumscription of subsections *Macrolonchium* and *Philodendron* (Croat, 1997). However, this character state is also found in species nested in other clades containing members of the series *Fibrosa* Croat within sect. *Philodendron* (e.g., *P. tenue* K. Koch & Augustin in clade 10, *P. grandipes* K. Krause in clade 11). Clade 6 (BS = 75, JK = 65, PP = 0.95) includes

epiphytes, appressed-climbing hemiepiphytes, and procumbent terrestrial species, all endemic to southeast Brazil (Sakuragui et al., 2005, 2011). Clade 7 (BS = 99, JK = 99, PP = 1.0) represents a group of appressed-climbing hemiepiphytes from the Amazon Basin and the Guianas with often three-lobed or deeply incised-lobate leaf blades (traditionally assigned to sect. *Polytomium* [Schott] Engl. or sect. *Schizophyllum* [Schott] Engl.) or at least with blades featuring well-developed posterior lobes (sect. *Philodendron*, the largest group within the subgenus).

Philodendron purulhense Croat is endemic to southern Mexico (Chiapas), Guatemala and Honduras (Croat, 1997) and was resolved sister to clades 8 and 9 (Fig. 2b). These two clades contain members from seven different sections, including the representatives of the small sections *Camptogynium* K. Krause, *Dolichogynium* Croat & Köster, and *Tritomophyllum*. As far as has been documented, most species in clades 8 and 9 are characterized by a solitary ovule per locule. Clade 8 (BS = 85, JK = 85, PP = 1.0) comprises mostly species distributed in the Amazon basin along with three species restricted to northern Venezuela (*P. fendleri* K. Krause) or the Guianas (*P. moonenii* Croat and *P.* cf. *pokigronense* Croat). Apart from *P. krugii* Engl. from Tobago and northern Venezuela (Engler, 1899), clade 9 (BS = 85, JK = 80, PP = 1.0) includes species occurring in Central America, the Chocó ecoregion, and the northern Andes.

Clades 10–14 (Fig. 2C) contain species mostly assigned to sect. *Macrobelium* and sect. *Philodendron* (Fig. 2C). Species of sect. *Macrobelium* have basal or sub-basal placentation and typically solitary or few ovules per locule, while species of sect. *Philodendron* are characterized by having axile placentation and many ovules per locule (Croat, 1997). Clade 10 (BS = 98, JK = 98, PP = 1.0) includes species mainly of sect. *Philodendron* and represents mostly those species with conspicuously velvety or at least completely matt adaxial leaf surfaces, which are often ornamented (mottled or with much paler veins). Apart from *P. ornatum*, which is widely distributed in South America, the species of this clade are restricted to the northern Andes and the Chocó ecoregion (with *P. verrucosum* L. Mathieu ex Schott reaching Costa Rica). Clade 11 (BS = 100, JK = 100, PP = 1.0) comprises three species from Central America and the Chocó ecoregion (Engler, 1905; Coelho et al., 2015). Clade 12 (BS = 87, JK = 85, PP = 1.0) comprises species occurring in northern South America with *P. lacerum* (Jacq.) Schott from the Greater Antilles (Schott, 1829; Acevedo-Rodríguez and Strong, 2012). Clade 13 (BS = 98, JK = 96, PP = 1.0) contains species endemic to the Chocó ecoregion recently described by Croat and Mora (2004) and Croat et al. (2016), whereas clade 14 (BS = 79, JK = 70, PP = 0.99) consists of members of sect. *Macrobelium* from Central America.

Time-calibrating the phylogenetic tree of *Philodendron*

Node ages estimated with the fossil+secondary calibration approach (using one fossil and a single secondary constraint) deviate from the ages estimated in Nauheimer et al. (2012) more than the ages calculated with three secondary calibration approach (Table 3). These discrepancies between the ages calculated with the fossil+secondary calibration approach and the ages previously reported by Nauheimer et al. (2012) might be explained by different factors. Secondary calibration points could only be applied to nodes that were well-supported in the Araceae fossil calibrated phylogeny by Nauheimer et al. (2012) and received statistical support in the present study. These correspond to three nodes: 28, 109, and 113 (Fig. 3; Appendix S2). In order to test a fossil-calibration approach, we included the closest outgroup taxon to *Philodendron* with a reliable fossil (*Montrichardia aquatica*; Herrera et al., 2008). However, this node is resolved sister to two of the three nodes (28 and 109) that could be used for secondary calibration points. Given the topological proximity between these nodes (Appendix S2), initial tests in divergence-time analyses (data not shown) revealed that it was not possible to combine all three secondary constraints and the fossil constraint since the priors applied to each node contradict one another. Therefore, in the fossil+secondary calibration approach it was possible to calibrate only two nodes: one fossil calibration for the lineage including *M. linifera* and one secondary calibration to node 113 (Table 2). The clade containing the taxon with a fossil record (*Montrichardia*+*Schismatoglottis*) in our study represents a much larger clade according to Nauheimer et al. (2012). Sparse taxon sampling affects age estimates, particularly in combination with a single fossil calibration (Schulte, 2013); therefore, the use of single species for a fossil calibration to represent larger clades in our outgroup may explain why the fossil+secondary-calibration approach resulted in younger ages, compared to the results in Nauheimer et al. (2012; Table 3). Furthermore, even though paleontological calibrations have been recommended for estimating evolutionary divergence times (Schenk, 2016), adding branches to the phylogeny in order to accommodate a fossil calibration when the focal group lacks paleontological evidence, as is the case with *Philodendron*, is more likely to bias divergence-time estimates than to accurately estimate the evolutionary history (Hipsley and Müller, 2014). Therefore, we focus our discussion on the ages obtained using the secondary calibration approach (Fig. 3 and Table 3).

Diversification history of *Philodendron* in the context of Neotropical plant evolution

Studies in other Neotropical species-rich lineages have corroborated either the "museum" model, with a steady and consistent accumulation of species diversity (e.g., Quiinoideae; Schneider and Zizka, 2017) or the cradle model, with higher diversification rates during short periods (e.g., *Inga*, Richardson et al., 2001; *Costus* subgenus *Costus*, Kay et al., 2005). The present study indicates that the diversification history of the genus *Philodendron* is a complex process characterized by a lineage-specific diversification rate shift within subgenus *Philodendron*. A recent acceleration in the diversification rate occurred in the species-rich and predominantly epiphytic lineage corresponding to subgenus *Philodendron* from 0.55 to 0.73 events/Ma/lineage from ~12 mya to the present (Fig. 4). In contrast, its sister lineage containing the subgenera *Meconostigma* and *Pteromischum* diversified at a relatively low, consistent diversification rate from 0.30 to 0.35 events/Ma/lineage since its origin ~22 mya to the present (Fig. 4). Based on the differences in the species diversification process between these sister lineages, we consider that a single model of diversification (cradle or museum) fails to explain the species diversification in *Philodendron*. Therefore, our results are more in line with the idea that high species diversity in Neotropical lineages such as *Philodendron* can be explained by periods of episodic species turnover or, in this case, a "burst" of species diversification for one lineage (Koenen et al., 2015; Pennington et al., 2015).

The recent geological dynamics in the Neotropics are likely to have been a driver of speciation in numerous plant lineages, including epiphytes, herbs, lianas, and trees (Hoorn et al., 2010; Antonelli and Sanmartín, 2011; Hughes et al., 2013; Lohmann et al., 2013;

Givnish et al., 2014). The origin of *Philodendron* co-occurred with the beginning of the mountain uplift of the central and northern Andes in the late Oligocene to the early Miocene. The uplift of the Andes coincides with the diversification of the first modern montane plant and animal genera in the Neotropics (~23 mya; Hoorn et al., 2010). Most *Philodendron* species arose within the past 10 Ma and are resolved within subgenus *Philodendron*, and this coincides with the most intense orogenic periods of the Andean region (~12 and ~4.5 mya; Hoorn et al., 2010). It is likely that the orogenic activity in the Andes during that period facilitated the diversification of *Philodendron* by creating new habitats (Antonelli and Sanmartín, 2011; Luebert and Weigend, 2014), as has been found in many other recently evolved Neotropical lineages, such as *Costus* (Kay et al., 2005), *Guarea* F. Allam. ex L. and *Trichilia* P. Browne (Koenen et al., 2015), *Guatteria* Ruiz & Pav. (Erkens et al., 2007), *Inga* (Richardson et al., 2001; Nicholls et al., 2015), *Renealmia* L. f. (Särkinen et al., 2007), Bromeliaceae (Givnish et al., 2014), and Orchidaceae (Givnish et al., 2015).

Croat (1997) indicated that widely distributed species of *Philodendron* may have strong dispersal abilities or an ancient origin, perhaps predating the Miocene and the Pliocene and, therefore, evolving over a longer period in which the species could have dispersed across broad geographic ranges. The oldest lineage within subgenus *Philodendron* diversified ~11 mya (clade 3; Table 3) and includes some of the most widespread species, in particular *P. hederaceum*, which occurs in the Greater Antilles and from Mexico throughout Central and South America (Croat, 1997; Figs. 2 and 3). However, our results indicate that some widely distributed species arose more recently, ~4 mya (*P. fragrantissimum* in clade 4 and *P. ornatum* in clade 10; Table 3; Figs. 2 and 3). Thus, widespread species are found both in older and in more recent clades, indicating that intrinsic factors such as dispersal abilities may have helped these widespread *Philodendron* species to colonize their habitats.

Within *Philodendron*, epiphytism is found almost exclusively in subgenus *Philodendron*, and its geographic diversity patterns resemble those found in other lineages that contain predominantly vascular epiphytes in the Neotropics. These epiphytic lineages constitute a major portion of the species richness in the Neotropical forests, especially lineages of the families Araceae, Bromeliaceae, Orchidaceae, and Polypodiaceae (Gentry and Dodson, 1987; Givnish et al., 2011, 2014; Zotz, 2013, 2016; Sundue et al., 2015). In contrast to the diversification history of ferns (Sundue et al., 2015), studies on bromeliads and orchids have shown that epiphytic lineages have higher net rates of diversification compared to their terrestrial relatives (Givnish et al., 2014, 2015). The epiphytic life form arose in the late Eocene in orchids and in the Miocene in bromeliads (Givnish et al., 2014, 2015). In the genus *Philodendron*, a lineage-specific diversification rate upshift occurred after the origin of the predominantly epiphytic subgenus *Philodendron* ~12 mya and it coincides with one of the most intense periods of mountain uplift in the Andes (Figs. 3 and 4). We therefore hypothesize that the high diversification rate in subgenus *Philodendron* compared to the other subgenera of *Philodendron* is associated with the colonization of perhumid forests in the Andes and their foothills that likely promoted the evolution of the epiphytic habit. However, this remains to be robustly tested, since understanding the epiphytism in *Philodendron* requires further morphological and ecological studies. In contrast to subgenus *Philodendron*, its sister lineage showed a low diversification rate (Figs. 1 and 4) and has gradually accumulated terrestrial species (subgenus *Meconostigma*) distributed in open environments in lowland forests in Amazonia and southeast Brazil, as well as vines (subgenus *Pteromischum*) occurring in the dense rainforests of Amazonia, the Chocó ecoregion, and Central America (Figs. 1 and 4). Although the taxon sampling for subgenera *Meconostigma* and *Pteromischum* is scarce, our study provides insights into the diversification history of a widely distributed angiosperm lineage in the Neotropics. We provide a robust phylogenetic framework and divergence-time estimates analysis to enable future testing of hypotheses that may explain the accelerated diversification rate within subgenus *Philodendron* compared to the rest of the genus *Philodendron*.

CONCLUSIONS

No section from the currently accepted infrageneric classification of subgenus *Philodendron* was recovered as monophyletic. The present study represents another example of a recent species radiation in the Neotropics that lends support to the global model of episodic periods of high species turnover (Koenen et al., 2015; Pennington et al., 2015) rather than endorsing the traditional models of diversification (cradle and museum models). Most of the species diversity in the genus *Philodendron* originated rapidly and recently within subgenus *Philodendron*. It will be beneficial to test the biotic and abiotic factors that may have influenced the speciation pattern found in *Philodendron*. The present study provides a basis for investigating the historical geographic ranges and the evolution of *Philodendron*, one of the most diverse genera in the Neotropical rainforests but one that is poorly understood.

ACKNOWLEDGMENTS

The authors thank the horticultural staff of the Botanic Garden and Botanical Museum Berlin (BGBM) and the Missouri Botanical Garden, St. Louis (MO), for successfully cultivating a large number of *Philodendron* species over many decades, thus safeguarding an invaluable resource for research. For providing further samples, we also thank the curators and gardeners of the Botanical Gardens of Bogotá and München; the Botanical Gardens of the Universities of Bonn, Göttingen, Potsdam, and Wien; the Palmengarten Frankfurt, and the Royal Botanic Gardens, Kew. J. Dietrich, J. Bansemer, D. Weigel, and K. Govers (BGBM) are acknowledged for technical assistance during the lab work. We thank an anonymous reviewer who provided invaluable comments on the manuscript. We are grateful to R. Cortés (Universidad Distrital Francisco José de Caldas, Bogotá) and M. Celis for supporting the fieldwork in Colombia, and the latter also for coordinating the scientific cooperation between the BGBM and the Botanical Garden of Bogotá. We further thank L. Palacios and F. Cardona (curators of the Herbario de la Universidad Tecnológica del Chocó [CHOCO] and the Herbario de la Universidad de Antioquia [HUA], respectively) and C. Kostelac (MO) for their dedicated support. We are indebted to the Verein der Freunde des Botanischen Gartens und Botanischen Museums Berlin-Dahlem e.V. for providing financial support for the fieldwork in Colombia. The Bundesministerium für Bildung und Forschung (BMBF) is especially acknowledged for funding a pilot project to facilitate scientific cooperation between Germany and Colombia (01DN13030). The first author thanks the Deutscher Akademischer Austauschdienst (DAAD) for providing a scholarship to carry out

his doctoral studies at the Freie Universität Berlin in the context of a program opened to doctoral students from Colombia.

DATA ACCESSIBILITY

Accessions and sequence data are available on the NBCI Sequence Read Archive (SRA).

SUPPORTING INFORMATION

Additional Supporting Information may be found online in the supporting information tab for this article.

LITERATURE CITED

Acevedo-Rodríguez, P., and M. T. Strong. 2012. Catalogue of seeds plants of the West Indies. Smithsonian Institution Scholarly Press, Washington, D.C., USA.

Alekseyenko, A. V., C. J. Lee, and M. A. Suchard. 2008. Wagner and Dollo: A stochastic duet by composing two parsimonious solos. *Systematic Biology* 57: 772–784.

Antonelli, A., and I. Sanmartín. 2011. Why are there so many plant species in the Neotropics? *Taxon* 60: 403–414.

Baele, G., and P. Lemey. 2013. Bayesian evolutionary model testing in the phylogenomics era: Matching model complexity with computational efficiency. *Bioinformatics* 29: 1970–1979.

Barabé, D., A. Bruneau, F. Forest, and C. Lacroix. 2002. The correlation between development of atypical bisexual flowers and phylogeny in the Aroideae (Araceae). *Plant Systematics and Evolution* 232: 1–19.

Barbosa, J. F., and C. M. Sakuragui. 2014. Taxonomy and conservation of the Brazilian extra-Amazonian species of *Philodendron* subg. *Pteromischum* (Araceae). *Phytotaxa* 191: 45–65.

Borsch, T., K. W. Hilu, D. Quandt, V. Wilde, C. Neinhuis, and W. Barthlott. 2003. Noncoding plastid *trnT-trnF* sequences reveal a well resolved phylogeny of basal angiosperms. *Journal of Evolutionary Biology* 16: 558–576.

Borsch, T., and D. Quandt. 2009. Mutational dynamics and phylogenetic utility of noncoding chloroplast DNA. *Plant Systematics and Evolution* 282: 169–199.

Bouckaert, R., J. Heled, D. Kuhnert, T. Vaughan, C. H. Wu, D. Xie, M. A. Suchard, et al. 2014. BEAST 2: A software platform for Bayesian evolutionary analysis. *Plos Computational Biology* 10.

Braucks Calazans, L. S., C. M. Sakuraguia, and S. J. Mayo. 2014. From open areas to forests? The evolutionary history of *Philodendron* subgenus *Meconostigma* (Araceae) using morphological data. *Flora* 209: 117–121.

Calazans, L. S. B., and C. M. Sakuragui. 2013. A new species of *Philodendron* (Araceae) and a key to Brazilian Atlantic forest species of *P.* subgenus *Pteromischum*. *Phytotaxa* 94: 49–55.

Campagna, M. L., and S. R. Downie. 1998. The intron in chloroplast gene *rpl16* is missing from the flowering plant families Geraniaceae, Goodeniaceae, and Plumbaginaceae. *Transactions of the Illinois State Academy of Science* 91: 1–11.

Carlsen, M., and T. B. Croat. 2013. A molecular phylogeny of the species-rich Neotropical genus *Anthurium* (Araceae) based on combined chloroplast and nuclear DNA. *Systematic Botany Monographs* 38: 576–588.

Coelho, M. A. N., M. L. Soares, L. S. B. Calazans, E. G. Gonçalves, I. M. Andrade, T. A. De Pontes, C. M. Sakuragui, et al. 2015. Araceae in lista de espécies da flora do Brasil. Flora do Brasil 2020. Available at http://floradobrasil.jbrj.gov.br/.

Condamine, F. L., N. S. Nagalingum, C. R. Marshall, and H. Morlon. 2015. Origin and diversification of living cycads: A cautionary tale on the impact of the branching process prior in Bayesian molecular dating. *Bmc Evolutionary Biology* 15: 65.

Couvreur, T. L. P., P. M. D., L. W. Chatrou, R. M. K. Saunders, Y. C. F. Su, J. E. Richardson, and R. H. J. Erkens. 2011. Early evolutionary history of the flowering plant family Annonaceae: Steady diversification and boreotropical geodispersal. *Journal of Biogeography* 38: 664–680.

Crisp, M. D., N. B. Hardy, and L. G. Cook. 2014. Clock model makes a large difference to age estimates of long-stemmed clades with no internal calibration: A test using Australian grasstrees. *Evolutionary Biology* 14: 1–17.

Croat, T. B. 1997. A revision of *Philodendron* subgenus *Philodendron* (Araceae) for Mexico and Central America. *Annals of the Missouri Botanical Garden* 84: 311–704.

Croat, T. B. 2013. *Philodendron joaosilvae*, a new species of *Philodendron*, subgenus *Philodendron*, section *Philodendron* (Araceae) from Brazil. *Aroideana* 36E: 92–99.

Croat, T. B., X. Delannay, S. Duncan, and C. V. Kostelac. 2016. Revision of *Philodendron* from the Lita-San Lorenzo region (Esmeraldas province, Ecuador). *Aroideana* 39: 26–315.

Croat, T. B., P. Huang, J. Lake, and C. V. Kostelac. 2010. Araceae of the flora of La Planada, Nariño department, Colombia. *Aroideana* 33: 75–142.

Croat, T. B., and M. M. Mora. 2004. New taxa of Araceae from Cabo Corrientes in Chocó department of Colombia. *Aroideana* 27: 90–129.

Cusimano, N., J. Bogner, S. J. Mayo, P. C. Boyce, S. Y. Wong, M. Hesse, W. L. A. Hetterscheid, et al. 2011. Relationships within the Araceae: Comparison of morphological patterns with molecular phylogenies. *American Journal of Botany* 98: 654–668.

Darriba, D., G. L. Taboada, R. Doallo, and D. Posada. 2012. jModelTest 2: More models, new heuristics and parallel computing. *Nature Methods* 9: 772.

Davis, C. C., C. O. Webb, K. J. Wurdack, C. A. Jaramillo, and M. J. Donoghue. 2005. Explosive radiation of Malpighiales supports a Mid-Cretaceous origin of modern tropical rain forests. *The American Naturalist* 165: 36–65.

Doyle, J. J., and J. L. Doyle. 1987. A rapid DNA isolation procedure for small quantities of fresh leaf tissue. *Phytochemical Bulletin* 19: 11–15.

Drew, B. T., and K. Sytsma. 2013. The South American radiation of *Lepechinia* (Lamiaceae): Phylogenetics, divergence times and evolution of dioecy. *Botanical Journal of the Linnean Society* 171: 171–190.

Droege, G., K. Barker, O. Seberg, J. Coddington, E. Benson, W. G. Berendsohn, B. Bunk, et al. 2014. The global genome biodiversity network (GGBN) data standard specification. *Nucleic Acids Research* 42(D1): D607–D612.

Drummond, A. J., and R. Bouckaert. 2015. Bayesian evolutionary analysis with BEAST. Cambridge University Press, Cambridge, UK.

Drummond, A. J., S. Y. W. Ho, M. J. Phillips, and A. Rambaut. 2006. Relaxed phylogenetics and dating with confidence. *PLoS Biology* 4: 699–710.

Drummond, A. J., M. A. Suchard, D. Xie, and A. Rambaut. 2012. Bayesian phylogenetics with BEAUti and the BEAST 1.7. *Molecular Biology and Evolution* 29: 1969–1973.

Engler, A. 1899. Beiträge zur Kenntnis der Araceae. IX. 16. Revision der Gattung *Philodendron* Schott. *Botanische Jahrbücher für Systematik, Pflanzengeschichte und Pflanzengeographie* 26: 509–564.

Engler, A. 1905. Beiträge zur Kenntnis der Araceae. X. 18. *Botanische Jahrbücher fur Systematik, Pflanzengeschichte und Pflanzengeographie* 37: 110–143.

Erkens, R. H. J., L. W. Chatrou, J. W. Maas, T. Van Der Niet, and V. Savolainen. 2007. A rapid diversification of rainforest trees (*Guatteria*; Annonaceae) following dispersal from Central into South America. *Molecular Phylogenetics and Evolution* 44: 399–411.

FitzJohn, R. G., W. P. Maddison, and S. P. Otto. 2009. Estimating trait-dependent speciation and extintion rates from incompletely resolved phylogenies. *Systematic Biology* 58: 595–611.

Forest, F. 2009. Calibrating the tree of life: Fossils, molecules and evolutionary timescales. *Annals of Botany* 104: 789–794.

Gascuel, O. 1997. BIONJ: An improved version of the NJ algorithm based on a simple model of sequence data. *Molecular Biology and Evolution* 14: 685–695.

Gauthier, M. P. L., D. Barabe, and A. Bruneau. 2008. Molecular phylogeny of the genus *Philodendron* (Araceae): Delimitation and infrageneric classification. *Botanical Journal of the Linnean Society* 156: 13–27.

Gentry, A. H., and C. H. Dodson. 1987. Diversity and biogeography of Neotropical vascular epiphytes. *Annals of the Missouri Botanical Garden* 74: 205–233.

Givnish, T. J., M. H. J. Barfuss, B. Van Ee, R. Riina, K. Schulte, R. Horres, P. A. Gonsiska, et al. 2011. Phylogeny, adaptative radiation, and historical biogeography in Bromeliaceae: Insights from an eight-locus plastid phylogeny. *American Journal of Botany* 98: 872–895.

Givnish, T. J., M. H. J. Barfuss, B. Van Ee, R. Riina, K. Schulte, R. Horres, P. A. Gonsiska, et al. 2014. Adaptative radiation, correlated and contingent evolution, and net species diversification in Bromeliaceae. *Molecular Phylogenetics and Evolution* 71: 55–78.

Givnish, T. J., D. Spalink, M. Ames, S. P. Lyon, S. J. Hunter, A. Zuluaga, W. J. D. Iles, et al. 2015. Orchid phylogenomics and multiple drivers of their extraordinary diversification. *Proceedings of the Royal Society B* 282: 20151553.

Govaerts, R., J. Bogner, J. Boos, P. Boyce, B. Cosgriff, T. B. Croat, E. Gonçalves, et al. 2017. World Checklist of Araceae. Facilitated by the Royal Botanic Gardens, Kew. http://wcsp.science.kew.org.

Grayum, M. H. 1996. Revision of *Philodendron* subgenus *Pteromischum* (Araceae) for Pacific and Caribbean tropical America. *Systematic Botany Monographs* 47: 1–233.

Herrera, F. A., C. A. Jaramillo, D. L. Dilcher, S. L., S. L. Wing, and C. Gómez-N. 2008. Fossil Araceae from a Paleocene Neotropical rainforest in Colombia. *American Journal of Botany* 95: 1569–1583.

Hilu, K. W., T. Borsch, K. Muller, D. E. Soltis, P. S. Soltis, V. Savolainen, M. W. Chase, et al. 2003. Angiosperm phylogeny based on *matK* sequence information. *American Journal of Botany* 90: 1758–1776.

Hipsley, C. A., and J. Müller. 2014. Beyond fossil calibrations: Realities of molecular clock practices in evolutionary biology. *Frontiers in Genetics* 5.

Hoorn, C., F. P. Wesselingh, H. Ter Steege, M. A. Bermudez, A. Mora, J. Sevink, I. Sanmartin, et al. 2010. Amazonia through time: Andean uplift, climate change, landscape evolution, and biodiversity. *Science* 330: 927–931.

Hughes, C. E., R. T. Pennington, and A. Antonelli. 2013. Neotropical plant evolution: Assembling the big picture. *Botanical Journal of the Linnean Society* 171: 1–18.

Kay, K. M., P. A. Reeves, R. G. Olmstead, and D. W. Schemske. 2005. Rapid speciation and evolution of humminbird pollination in neotropical *Costus* subgenus *Costus* (Costaceae): Evidence from nrDNA ITS and ETS sequences. *American Journal of Botany* 92: 1899–1910.

Kelchner, S. A. 2002. Group II introns as phylogenetic tools: Structure, function, and evolutionary constraints. *American Journal of Botany* 89: 1651–1669.

Klimko, M., M. Wawrzyńska, and J. Wiland-Szymańska. 2014. Comparative leaf morphology and anatomy of some Neotropical *Philodendron* Schott (Araceae) species. *Steciana* 18: 159–171.

Koenen, E. J. M., J. J. Clarkson, T. D. Pennington, and L. W. Chatrou. 2015. Recently evolved diversity and convergent radiations of rainforest mahoganies (Meliaceae) shed new light on the originsof rainforest hyperdiversity. *New Phytologist* 207: 327–339.

Köster, N., and T. B. Croat. 2011. A new section and a new species of *Philodendron* (Araceae) from Ecuador. *Willdenowia* 41.

Krause, K. 1913. Araceae-Philodendroideae-Philodendreae-Philodendrinae. Engler, A. and K. Krause [eds.], Das Pflanzenreich Regni Vegetabilis Conspectus. W. Engelmann, Leipzig, Germany. IV: 1–143.

Lohmann, G. L., D. C. Bell, F. M. Calio, and C. R. Winkworth. 2013. Pattern and timing of biogeographical history in the Neotropical tribe Bignonieae (Bignoniaceae). *Botanical Journal of the Linnean Society* 171: 155–170.

Löhne, C., and T. Borsch. 2005. Molecular evolution and phylogenetic utility of the *petD* group II intron: A case study in basal angiosperms. *Molecular Biology and Evolution* 22: 317–332.

Loss-Oliveira, L., C. Sakuragui, M. De Lourdes Soares, and C. G. Schrago. 2016. Evolution of *Philodendron* (Araceae) species in Neotropical biomes. *Peerj* 4: 1–18.

Luebert, F., and M. Weigend. 2014. Phylogenetic insights into Andean plant diversification. *Frontiers in Ecology and Evolution* 2: 1–17.

Mayo, S. J. 1986. Systematics of *Philodendron* Schott (Araceae) with special reference to inflorescence characters. Ph.D. dissertation, University of Reading, Reading, UK.

Mayo, S. J. 1988. Aspectos da evolução e da geografia do gênero *Philodendron* Schott (Araceae). *Acta Botanica Brasilica* 1: 27–40.

Mayo, S. J. 1989. Observations of gynoecial structure in *Philodendron* (Araceae). *Botanical Journal of the Linnean Society* 100: 139–172.

Mayo, S. J. 1991. A revision of *Philodendron* subgenus *Meconostigma* (Araceae). *Kew Bulletin* 46: 601–681.

Mayo, S. J., J. Bogner, and P. C. Boyce. 1997. The genera of Araceae. The Trustees, Royal Botanic Gardens, Kew, UK.

Mckenna, D. D., and B. D. Farrell. 2006. Tropical forests are both evolutionary cradles and museums of leaf beetle diversity. *Proceedings of the National Academy of Sciences USA* 103: 10947–10951.

Messing, J. 1983. New M13 vectors for cloning. *Methods in Enzymology* 101: 20–78.

Miller, M. A., W. Pfeiffer, and T. Schwartz. 2010. Creating the CIPRES science gateway for inference of large phylogenetic trees. *In* Proceedings of the Gateway Computing Environments Workshop (GCE). IEEE Press, Piscataway, New Jersey, USA. pp. 1–8.

Moore, B. R., S. Höhna, M. R. May, B. Rannala, and J. P. Huelsenbeck. 2016. Critically evaluating the theory and performance of Bayesian analysis of macroevolutionary mixtures. *Proceedings of the National Academy of Sciences USA* 113: 9569–9574.

Müller, K. 2004. PRAP-computation of Bremer support for large data sets. *Molecular Phylogenetics and Evolution* 31: 780–782.

Müller, K. 2005. SeqState—primer design and sequence statistics for phylogenetic DNA data sets. *Applied Bioinformatics* 4: 65–69.

Müller, K., D. Quandt, J. Müller, and C. Neinhuis. 2005. PhyDE, version 0.92: Phylogenetic data editor. http://www.phyde.de.

Nauheimer, L., D. Metzler, and S. S. Renner. 2012. Global history od the ancient monocot family Araceae inferred with models accounting for past continental positions and previous ranges based on fossils. *New Phytologist* 195: 938–950.

Neupane, S., P. O. Lewis, S. Dessein, H. Shanks, S. Paudyal, and F. Lens. 2017. Evolution of woody life form on tropical mountains in the tribe Spermacoceae (Rubiaceae). *American Journal of Botany* 104: 419–438.

Nicholls, J. A., R. T. Pennington, E. J. M. Koenen, C. E. Hughes, J. Hearn, L. Bunnefeld, K. G. Dexter, et al. 2015. Using targeted enrichment of nuclear genes to increase phylogenetic resolution in the Neotropical rain forest genus *Inga* (Leguminosae: Mimosoideae). *Frontiers in Plant Science* 6: 1–20.

Nixon, K. C. 1999. The parsimony ratchet, a new method for rapid parsimony analysis. *Cladistics* 15: 407–414.

Pennington, R. T., M. Hughes, and P. W. Moonlight. 2015. The origins of tropical rainforest hyperdiversity. *Trends in Plant Science* 20: 693–695.

Plummer, M., N. Best, K. Cowles, and K. Vines. 2006. CODA: Convergence diagnosis and output analysis for MCMC. *R News* 6: 7–11.

Rabosky, D. L. 2014. Automatic detection of key innovations, rate shifts, and diversity-dependence on phylogenetic trees. *PLoS One* 9: e89543.

Rabosky, D. L., M. Grundler, C. Anderson, P. Title, J. Shi, H. Huang, J. W. Brown, and J. Larson. 2014. BAMMtools: An R package for the analysis of evolutionary dynamics on phylogenetic trees. *Methods in Ecology and Evolution* 5: 701–707.

Rabosky, D. L., J. S. Mitchell, and J. Chang. 2017. Is BAMM flawed? Theoretical and practical concerns in the analysis of multi-rate diversification models. *Systematic Biology* 66: 477–498.

Rambaut, A. 2012. FigTree version 1.4: Molecular evolution, phylogenetics and epidemiology. University of Edinburgh, Institute of Evolutionary Biology, Edinburgh, UK.

R Core Team. 2013. R: A language and environment for statistical computing. R Foundation for Statistical Computing, Vienna, Austria. http://www.R-project.org/.

Richardson, J. E., R. T. Pennington, T. D. Pennington, and P. M. Hollingsworth. 2001. Rapid diversification of a species-rich genus of Neotropical rain forest trees. *Science* 293: 2242–2245.

Ronquist, F., and J. P. Huelsenbeck. 2003. MrBayes 3: Bayesian phylogenetic inference under mixed models. *Bioinformatics* 19: 1572–1574.

Ronquist, F., J. P. Huelsenbeck, and M. Teslenko. 2011. MrBayes version 3.2 Manual: Tutorials and model summaries. http://mrbayes.sourceforge.net/mb3.2_manual.pdf.

Saitou, N., and M. Nei. 1987. The neighbor-joining method: A new method for reconstruction of phylogenetic trees. *Molecular Biology and Evolution* 4: 406–425.

Sakuragui, C. M., L. S. Braucks Calazans, É. Barroso De Morais, M. A. Nadruz Coelho, and M. O. De Oliveira Pellegrini. 2011. Diversity and conservation of *Philodendron* Schott (Araceae) in Atlantic forest of Rio de Janeiro state, Brazil. *Feddes Repertorium* 122: 472–496.

Sakuragui, C. M., S. J. Mayo, and D. C. Zappi. 2005. Taxonomic revision of Brazilian species of *Philodendron* section *Macrobelium*. *Kew Bulletin* 60: 465–513.

Särkinen, T. E., M. F. Newman, P. J. M. Maas, H. Maas, A. D. Poulsen, D. J. Harris, J. E. Richardson, et al. 2007. Recent oceanic long-distance dispersal and divergence in the amphi-Atlantic rain forest genus *Renealmia* L.f. (Zingiberaceae). *Molecular Phylogenetics and Evolution* 44: 968–980.

Schenk, J. J. 2016. Consequences of secondary calibrations on divergence time estimates. *PLoS One* 11: e0148228.

Schneider, J. V., and G. Zizka. 2017. Phylogeny, taxonomy and biogeography of Neotropical Quiinoideae (Ochnaceae s.l.). *Taxon* 66: 855–867.

Schott, H. W. 1829. Für Liebhaber der Botanik. *Wiener Zeitschrift für Kunst, Literatur, Theater und Mode* 1829(3): 779–780.

Schott, H. W. 1856. Synopsis Aroidearum. Typis Congregationis Mechitharisticae, Vienna.

Schulte, J. A., II. 2013. Undersampling taxa will underestimate molecular divergence dates: An example from the South American lizard clade Liolaemini. *International Journal of Evolutionary Biology* ID 628467.

Shaul, S., and D. Graur. 2002. Playing chicken (*Gallus gallus*): Methodological inconsistencies of molecular divergence date estimates due to secondary calibration points. *Gene* 300: 59–61.

Shaw, J., E. B. Lickey, J. T. Beck, S. B. Farmer, W. Liu, J. Miller, K. C. Siripun, et al. 2005. The tortoise and the hare II: Relative utility of 21 noncoding chloroplast DNA sequences for phylogenetic analysis. *American Journal of Botany* 92: 142–166.

Shi, J. J., and D. L. Rabosky. 2015. Speciation dynamics during the global radiation of extant bats. *Evolution* 69: 1528–1545.

Silvestro, D., and I. Michalak. 2012. raxmlGUI: A graphical front-end for RAxML. *Organisms Diversity & Evolution* 12: 335–337.

Simmons, M. P., and J. V. Freudenstein. 2011. Spurious 99% bootstrap and jackknife support for unsupported clades. *Molecular Phylogenetics and Evolution* 61: 177–191.

Simmons, M. P., and H. Ochoterena. 2000. Gaps as characters in sequence-based phylogenetic analyses. *Systematic Biology* 49: 369–381.

Stöver, B. C., and K. F. Müller. 2010. TreeGraph 2: Combining and visualizing evidence from different phylogenetic analyses. *BMC Bioinformatics* 11: 7.

Sundue, M. A., W. L. Testo, and T. A. Ranker. 2015. Morphological innovation, ecological, opportunity, and the radiation of a major vascular epiphyte lineage. *Evolution* 69: 2482–2495.

Swofford, D. L. 2003. PAUP*: Phylogenetic analyses using parsimony (*and other methods). Sinauer Associates, Sunderland, Massachusetts, USA.

Wicke, S., and D. Quandt. 2009. Universal primers for the amplification of the plastid *trn*K/*mat*K region in land plants. *Anales del Jardín Botánico de Madrid* 66: 285–288.

Wong, S. J., T. P. Jean, N. K. Kiaw, A. S. Othman, H. L. Boon, B. F. Ahmad, and C. P. Boyc. 2013. Phylogeny of Asian *Homalomena* (Araceae) based on the ITS region combined with morphological and chemical data. *Systematic Botany Monographs* 38: 589–599.

Wong, S. J., A. W. Meerow, and T. B. Croat. 2016. Resurrection and new species of the Neotropical genus *Adelonema* (Araceae: Philodendron clade). *Systematic Botany* 41: 32–48.

Woodhams, M., D. A. Steane, R. C. Jones, D. Nicolle, V. Moulton, and B. R. Holland. 2013. Novel distances for Dollo data. *Systematic Biology* 62: 62–77.

Xie, W., P. O. Lewis, Y. Fan, L. Kuo, and M.-H. Chen. 2011. Improving marginal likelihood estimation for Bayesian phylogenetic model selection. *Systematic Biology* 60: 150–160.

Zotz, G. 2013. The systematic distribution of vascular epiphytes—a critical update. *Botanical Journal of the Linnean Society* 171: 453–481.

Zotz, G. 2016. Plants on Plants. The Biology of Vascular Epiphytes, Berlin Heidelberg New York, Springer.